2016-01-01

Case Studies In Implementing Intelligent Compaction In Construction Of Earthwork

Jorge Alberto Beltran
University of Texas at El Paso, jabeltran2@miners.utep.edu

CASE STUDIES IN IMPLEMENTING INTELLIGENT COMPACTION IN CONSTRUCTION OF EARTHWORK

JORGE ALBERTO BELTRAN VALENZUELA

Master's Program in Civil Engineering

APPROVED:

Soheil Nazarian, Ph.D., co-Chair

Mehran Mazari, Ph.D., co-Chair

Imad Abdallah, Ph.D.

Vladik Kreinovich, Ph.D.

Charles Ambler, Ph.D.
Dean of the Graduate School

Dedication

I would like to dedicate this thesis to my parents and my brother.

IMPROVING CONSTRUCTION QUALITY OF PAVEMENT GEOMATERIAL LAYERS USING INTELLIGENT COMPACTION DATA

by

JORGE ALBERTO BELTRAN VALENZUELA, BSCE

THESIS

Presented to the Faculty of the Graduate School of

The University of Texas at El Paso

in Partial Fulfillment

of the Requirements

for the Degree of

MASTER OF SCIENCE

Department of Civil Engineering

THE UNIVERSITY OF TEXAS AT EL PASO

August 2016

Acknowledgements

I would like to express my sincere appreciation to my thesis and project advisor, Dr. Soheil Nazarian for all his guidance throughout these years. Without his faith in me and advice, this would not have been possible. I would also like to thank Dr. Imad Abdallah for providing me the opportunity to work at the Center for Transportation Infrastructure Systems (CTIS). I want to express my gratefulness to Dr. Mehran Mazari who, while being miles away, provided his unconditional support, helped me develop most of my analytical skills and guided me throughout the project. Special thanks to Dr. Cesar Tirado for his mentorship in the programming portion of the project. I would also like to express my appreciation to Dr. Raed AlDouri for his assistance in geospatial analysis. I would also like to thank my thesis committee member, Dr. Vladik Kreinovich, for taking the time to review this thesis.

I would like to express my gratitude to the CTIS laboratory manager, Mr. Jose Garibay, for providing me with the help I needed. Finally, I would like to thank CTIS fellow graduate students Luis Lemus and Yahir Morales who have helped me in most parts of this research.

During the development of this project, I had the opportunity to collaborate with a number of professionals in Texas Department of Transportation. I would like to extend my gratitude to Dr. Jimmy Si, Mr. Richard Izzo, Mr. Wade Blackmon and Mr. Jaime Aparicio for their help and support.

I am very grateful to Dr. Anjan Kumar Siddagangaiah, a mentor and a friend who helped me during my starting days at the CTIS. I also want to thank my friends Ramon Cardona, Alejandro Miramontes, Enrique Guizar, Miguel Perez, Victor Garcia, Nancy Aguirre, Andrea Gutierrez and

Estefany Ramos for their unconditional support, great support and advice during those times I needed them the most.

Finally, I would like to thank and dedicate this thesis to my family: my father, Eprain Leonel Beltran Navarro, my mother, Alba Lorenia Valenzuela Clark, and my brother, Eprain Leonel Beltran Valenzuela for their uninterrupted support and motivation to obtain everything.

Abstract

The nuclear density gauge (NDG) is the current tool for field compaction quality control (QC) and quality assurance (QA) for soil and base layers in the state of Texas. The Texas Department of Transportation (TxDOT) uses this nondestructive testing (NDT) device to determine the compacted density and moisture content of earthwork and unbound aggregates. However, to provide the missing link between design and quality management parameters, an alternative stiffness-based approach would be more desirable. Intelligent Compaction (IC) is defined as continuous assessment of mechanistic soil properties (stiffness, modulus) through roller parameters (frequency, amplitude and speed) integrated with global positioning system (GPS) to provide a complete compaction and geographic information. TxDOT has currently defined proof mapping with an IC roller as an approximate way of assessing the uniformity of the compacted geomaterial. IC rollers can identify less stiff areas and significantly improve uniformity of compaction. A rigorous analysis of IC data was carried out to evaluate the compaction quality management of unbound pavement layers in the state of Texas.

Table of Contents

List of Tables

List of Figures

Chapter 1: Introduction

1.1 PROBLEM STATEMENT

The nuclear density gauge (NDG) is the current practice for field compaction quality control (QC) and quality assurance (QA) for soil and base layers in the state of Texas. The Texas Department of Transportation (TxDOT) uses this nondestructive testing (NDT) device to determine the dry density and moisture content of compacted earthwork and unbound aggregates. Since, stiffness parameters are more correlated to pavement design process, stiffness-based devices, such as the lightweight deflectometer (LWD), are recommended to replace density measurements. However, spot tests represent less than one percent of the compacted area, which leads to a lack of assessing the quality and uniformity of compaction in a continuous manner.

Continuous assessment of mechanistic soil properties (stiffness, modulus) through roller parameters (frequency, amplitude and speed) integrated with global positioning system (GPS) to provide a complete compaction and geographic information is "intelligent compaction (IC)" (Mooney et al., 2010). Two types of IC rollers are available in the market. One is the original equipment manufacturer (OEM) IC rollers and the other one is the retrofitted rollers. A number of roller manufacturers have implemented IC technology in their compaction equipment for both the hot mix asphalt (HMA) and soils. Each of these OEM systems employs different instrumentation to collect vibration data and use different methods to estimate the stiffness of the compacted layer. As an alternative option to an OEM system, a retrofit system (after-market kit) can be installed on a regular roller to collect IC data more economically.

TxDOT has currently specified proof mapping as an approximate way of assessing the uniformity of the compacted geomaterial. Intelligent compaction rollers can identify less-stiff

areas and significantly improve uniformity by proof mapping after completing the compaction process. For this thesis, a rigorous analysis of IC data for different geomaterial layers and number of roller passes was carried out to evaluate the responses of the soil. Alternative data interpretation methods were investigated to improve the repeatability of IC results. The alternative approach was investigated using different interpolation and geospatial methods. This thesis was carried out as part of two research projects. The first project that was sponsored by the Federal Highway Administration (FHWA) through TxDOT is entitled as "Intelligent Compaction Roller Retrofit Kit Validation." The second research project that was sponsored by TxDOT is entitled "Implementation of Intelligent Compaction Technology for Improving Compaction Quality of Soil and Base in Texas." This thesis includes the process of investigating alternative data interpretation methods and the performance of IC data in between layers/passes.

1.2 ORGANIZATION OF REPORT

Aside from the current chapter, this thesis consists of six additional chapters. Chapter 2 includes a brief review of the intelligent compaction system and the retrofit kits as well as the definition of the different IC measurement values.

Chapter 3 summarizes the process of data collection during the implementation of IC in the participating TxDOT districts. This includes the selection of the test sections, spot tests, IC data collection, GPS calibration and geospatial analysis processes. This chapter also includes the details of the UTEP instrumentation that was employed to validate the collected IC data in selected test sections.

Chapter 4 outlines the initiation and development of a comprehensive IC database and its elements during implementation of IC in TxDOT districts. Chapter 5 presents a summary of field

observations during the visits to the participating districts. These include the spot tests and IC roller measurements. Chapter 6 discusses the results of the field test for different IC rollers as well as the data collected by the UTEP validation system in Cleburne, TX.

Chapter 7 includes the conclusion and recommendations for the implementation of IC data.

Appendix A contains the detailed field observations during the implementation of IC during the construction of State Highway (SH) 24 is Paris District, TX. Appendix B is dedicated to the detailed IC data collection process and analysis during the IC evaluation in Cleburne, TX.

Chapter 2: Literature Review

2.1 INTRODUCTION

Intelligent Compaction is an emerging technology for monitoring the compaction process for HMA, base and soil layers and for managing the compaction data to improve the quality of compacted layers and to avoid under/over compaction. The advantages of intelligent compaction are reported as (Mooney et al. 2010, White and Vennapusa 2010):

- Improved quality and uniformity of compaction
- Reduced over/under compaction
- Identification of soft or weak spots

The following section contains a literature survey of the IC retrofit kit, IC measurement values (ICMVs) and their definitions.

2.2 INTELLIGENT COMPACTION RETROFIT KIT

Intelligent compaction is a specific terminology for a wider concept of continuous compaction control (CCC) that was initiated in Swedish Highway Administration in 1974. In 1975, Geodynamik was founded to continue the development of roller-mounted compaction meter. Geodynamik and Dynapac introduced the Compaction Meter Value (CMV) to monitor the roller-integrated compaction process (Thurner and Forsblad, 1978; Thurner and Sandström, 1980). In 1982, Bomag introduced the Omega value (which was a measure of compaction energy and time) and Terrameter (Ferris, 1985). With the introduction of mechanistic and performance-related soil properties, Bomag launched the Vibration Modulus that was a measure of dynamic soil stiffness (Floss et al. 2001; Kröber et al. 2001). In 1999, Ammann introduced the Soil Stiffness Parameter

followed by initiation of Compaction Control Value (CCV) by SAKAI in 2004 (Anderegg and Kaufmann 2004; Anderegg 1998). The IC systems have been under continuous development since then. Even though the IC systems were considered Original Equipment Manufacturer (OEM) systems, Trimble introduced the IC retrofit (after-market) kit to be installed on any regular vibratory roller to collect IC data. With the advancement and improvement of the IC retrofit kit, its application has been growing during the past couple of years. Due to the increasing application of the IC retrofit kits, there was a need to evaluate their performance during actual compaction process. This study was aimed to address the need to such evaluations.

2.3 INTELLIGENT COMPACTION MEASUREMENT VALUES

The concept of correlating stiffness of the compacted layer to the excitation frequency (Mooney and Adam, 2007) initiated the use of accelerometers to monitor the compaction process. This idea was further improved and became the basis of measurement for some of the roller vendors. Caterpillar (CAT) uses this concept as Compaction Meter Value (CMV) while HAMM utilizes that as HAMM Measurement Value (HMV). These measurement values are defined as (Mooney et al, 2010):

$$\boldsymbol{CMV} = \mathbf{300} \times \left(\frac{\boldsymbol{A_4}}{\boldsymbol{A_2}}\right) \tag{2.3.1}$$

where A2 is the acceleration of the forcing component of the vibration and A4 is the acceleration of the first harmonic of the vibration. As indicated in Figure 2.3.1, the CMV only takes the forcing frequency and first harmonic into account. However, if the compacted layer becomes stiffer, the other harmonics (A1 through A6 in Figure 2.3.2) could also be identified during the compaction process.

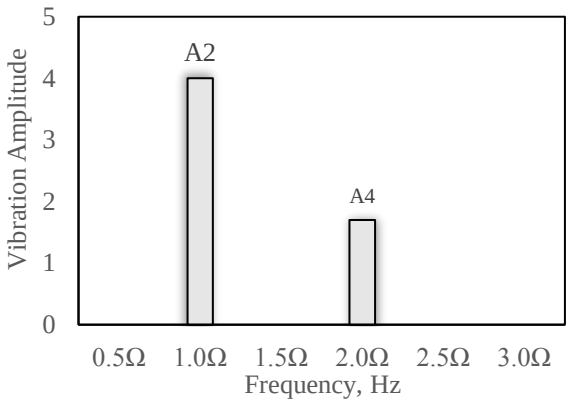

Figure 2.3.1: Forcing frequency and vibration harmonics for a soft layer (Nazarian et al, 2015)

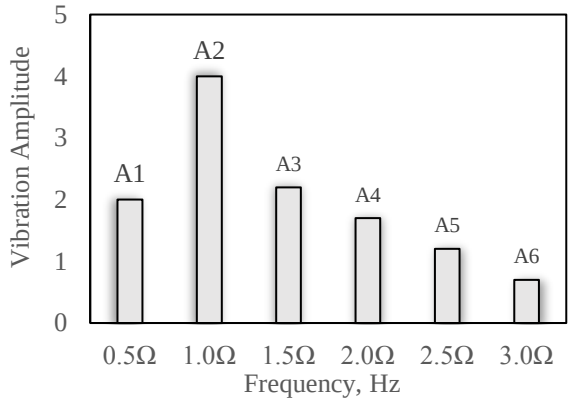

Figure 2.3.2: Forcing frequency and vibration harmonics for a stiff layer (Nazarian et al, 2015)

The SAKAI Compaction Control Value (CCV) utilizes the following equation to estimate the layer stiffness:

$$CCV = 100 \times \left[\frac{A_1+A_3+A_4+A_5+A_6}{A_1+A_2}\right] \quad (2.3.2)$$

Assuming that the rotational frequency of the forcing mode of the vibration is Ω, parameters A_1 through A_6 in equation 2.3.2 represent the acceleration of vibration at 0.5Ω, Ω, 1.5Ω, 2Ω, 2.5Ω and 3Ω, respectively.

2.4 GEOSTATISTICS IN INTELLIGENT COMPACTION

Geostatistics is a collection of techniques used to analyze and predict values for spatial attributes. The steps involved in geostatistical analysis are: (i) obtaining the variogram, a graph

which relates the variance at pairs of sample points to the separation distance between those pairs, (ii) fitting the model, and (iii) using the variogram model to predict the unsampled locations by using Kriging method or conditional simulation. Kriging or Gaussian process regression is a geostatistical method used for spatial interpolation. Unlike other interpolation methods, Kriging has the capability to assess the quality of the prediction with estimated errors. The variogram model is then used to measure spatially correlated component or spatial dependence. This produces an optimal unbiased estimate of the property across the entire spatial domain. The same procedure can be followed to interpolate through time with temporal data, such as, hourly or daily property measures. Geostatistical analyses also provide tools for spatial data exploration, identification of data anomalies, evaluation of errors in prediction of surface models, statistical estimation and optimal surface creation.

Significant amount of research has been conducted in using geostatistics for evaluating the compaction quality. Table 2.4.1 provides a summary of the studies conducted in the use of geostatistics for intelligent compaction. Unlike spot testing, geostatistics in IC as a quality assurance/quality control (QA/QC) tool for the use in compacted soil have the capability to demonstrate the spatial variability of compaction and depict soft or hard spot areas that can be targeted for repeated compaction. Studies conducted by White et al. (2008), Vennapusa et al. (2009) and White et al. (2011) have demonstrated the importance of conducting spatial analysis using geostatistics techniques rather than univariate statistics which can improve the visualization of the compaction non-uniformity. Vennapusa et al. (2009) demonstrated the use of variogram analysis in combination with conventional statistical analysis to effectively address the issue of non-uniformity in QA/QC during earthwork construction.

Table 2.4.1: Geostatistics in Intelligent Compaction (Siddagangaiah et al. 2013)

Reference	Objective and scope	Key findings/comments
White et al., 2007	Evaluated the utilization of intelligent compaction monitoring for unbound materials in the field. Test sections with different site conditions, rollers with different data measurements and storage system were evaluated.	Study demonstrated the use of variogram models to effectively characterize the uniformity of compaction by quantifying spatial variability. The study showed that the range from a variogram plot can be potentially used as a maximum separation distance between spot tests measurements. Also study showed that to reduce any significant error, roller measurement values from the middle of drum shall be considered.
Petersen et al., 2007	Evaluated the application of geostatistical tools to judge the adequacy of compaction and uniformity, assisting in the QC/QA process.	Traditional descriptive statistics were found to be inadequate to address the concern of uniform compaction. The use of IC data and geostatistics help to identify and fix the problematic areas of poor compaction, which in turn improve the overall life cycle of pavements.
White et al., 2008	To characterize the uniformity of the compacted soil layer using intelligent compaction technology with variable feedback control.	Findings from the study showed the limitations of univariate analysis in determining the uniformity of the compacted soil layer. Study identified the use of variogram model parameters to characterize the uniformity of compacted soil layer.
Vennapusa et al., 2009	To quantify the non-uniformity using spatial referenced roller measurements	Non-uniformity of compaction which cannot be explained with univariate analysis of roller measurements can be dealt with variogram analysis. Geostatistics can used to identify the areas of poor compaction and non-uniform conditions
White et al., 2011	Review of the field assessment studies and examined factors influencing the roller measurement values, correlations between the spot test measurements and spatial uniformity.	Geostatistical analysis of roller measurement values facilitate construction process control and characterize variations and non-uniformity.

White et al. (2008) reported that variograms developed for two different spatial areas with similar univariate statistics (i.e., mean and standard deviation) showed distinctly different shapes of variograms with different spatial statistics, which illustrate the importance of spatial modeling to characterize better the "non-uniformity" compared to using univariate statistics. This emphasizes the importance of dealing with "non-uniformity" in a spatial perspective rather than in a univariate statistics perspective.

FHWA recommends the use of Veda (a.k.a., Veta), a software developed to analyze data collected from GPS and roller monitoring. Veda displays simple statistical graphs like a histogram of RMVs (Figure 2.4.1) and semivariogram (Figure 2.4.2) and spatial distribution of RMCs (Figure 2.4.3). The data can also be imported into GIS software like ArcGIS and analyzed by using both spatial analysis tools and geostatistical tools.

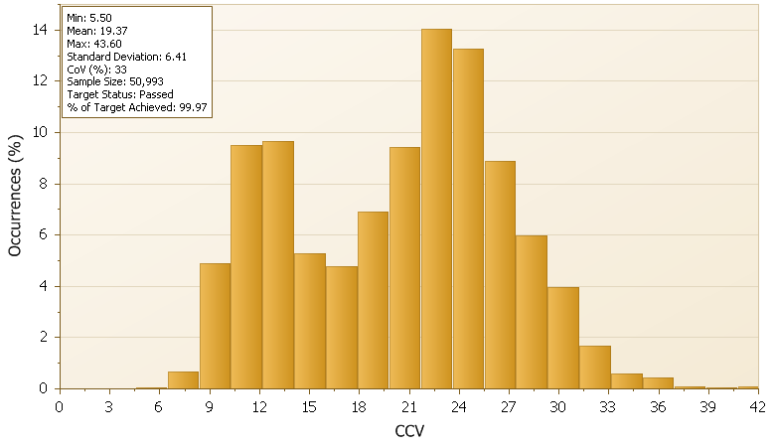

Figure 2.4.1: A histogram showing CCV Values and their occurrence in IC data with descriptive statistics (VETA v2) (Siddagangaiah et al. 2013)

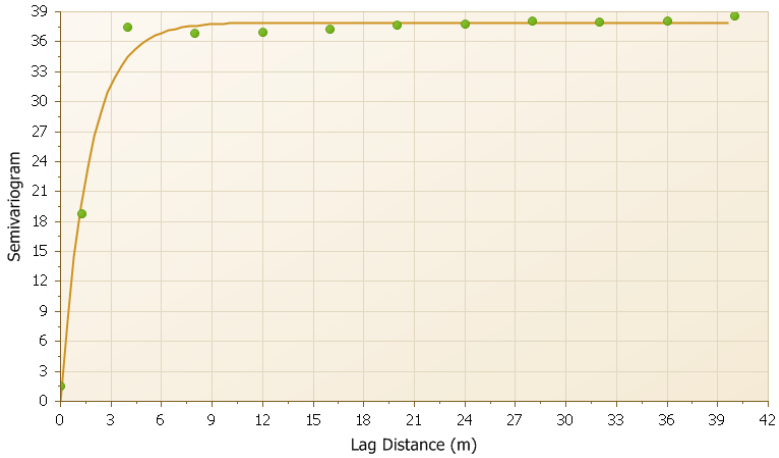

Figure 2.4.2: A semivariogram of CCV data (VETA v2) (Siddagangaiah et al. 2013)

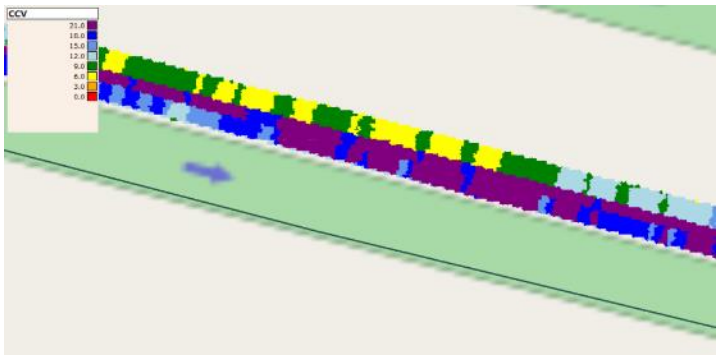

Figure 2.4.3: A color-coded map showing spatial variations in the CCV values (VETA v2) (Siddagangaiah et al. 2013)

Chapter 3: Data Collection

This chapter summarizes the typical test section and the location of the spot tests. Also, it refers to the different NDTs employed in this research, the possible correlations between the NDT and IC data, and a data acquisition system developed by UTEP research team

3.1 SPOT TESTS

The research team has been assisting the engineers and contractors with the IC data collection process. Figure 3.1.1 illustrates the schematic of a typical test section and spot test grid. As a part of this activity and to investigate the possible correlations between the conventional NDT spot tests and IC data, a test section was identified within a construction site in Paris District. The test section was marked for at least 30 test points by the research team to perform the spot test.

The following spot tests were performed on the compacted section at specified test points:

Falling Weight Deflectometer (FWD), is a nondestructive method considered to approximate the material properties that are compatible with loads exerted by traffic when deployed on top of the finished pavement. The FWD measures the pavement deflection at seven to nine points (with 12 in. offset) for a given load. The pavement layer parameters, FWD load and measured deflections are employed to backcalculate the stiffness of different pavement layers.

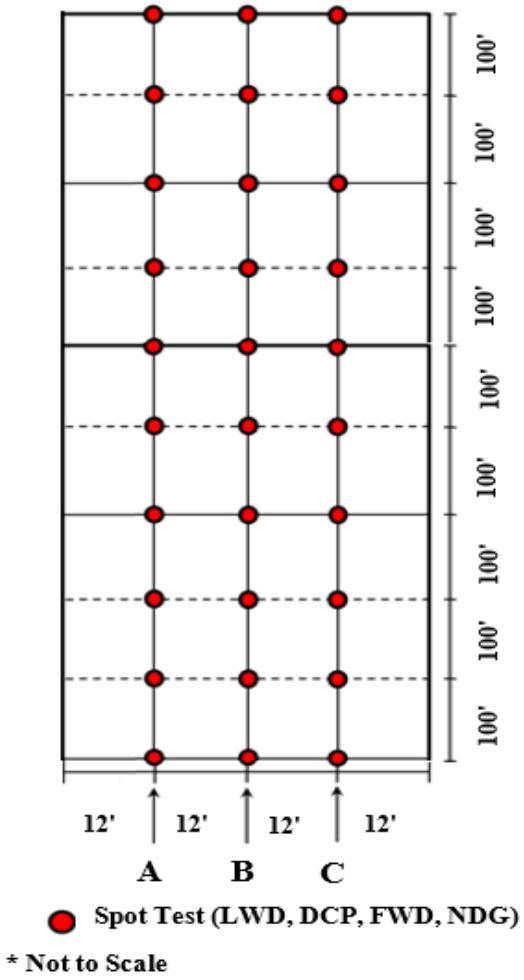

Figure 3.1.1: Schematic of the typical test section and location of spot tests.

Figure 3.1.2: Falling Weight Deflectometer (FWD)

Light Weight Deflectometer (LWD) is a portable version of FWD that has been developed as an alternative in-situ testing device to the plate load test. LWD imparts an impulse load through a load plate, and measures the deflection of either the soil surface or of the load plate itself, through a displacement sensor. Similar to FWD, the LWD determines the stiffness of the pavement system by measuring the material's response under the impact of a load with a known magnitude and dropped from a known height. LWD reports the composite modulus of the layers with the estimated depth of influence of up to several feet (Tirado et al, 2015). The LWD tests were performed in this project following the ASTM E2583. Three seating drops of the LWD loading weight should be followed by three measurement drops. Table 3.1.1 summarizes the specification of the two different models used in this study.

Figure 3.1.3: Light Weight Deflectometer (LWD)

Table 3.1.1: Specification of Lightweight Deflectometers.

Vendor/ Manufacturer	ZORN Instruments	ZORN Instruments
		
Model	LWD 2000	LWD 3.0
Plate Diameter	200 mm	300 mm
Mass of Falling Weight	10 kg	10 kg

Dynamic Cone Penetrometer (DCP) test involves driving a cone shaped probe into the soil or aggregate layer using a dynamic load and measuring the advancement of the device for each applied blow or interval of blows. The depth of penetration is directly impacted by the drop height, the weight, cone size, and cone shape. Moreover, the resistance to penetration is dependent on the shear strength of the material. The strength, in turn, is dependent on the density, moisture content, and material type. The ASTM D6951 process was followed to perform DCP tests during field evaluation to estimate the California Bearing Ratio (CBR) from the DCP penetration index. The TRL's recommended equation was employed to estimate modulus using the CBR values (Nazarian et al, 2015).

Figure 3.1.4: Dynamic Cone Penetrometer (DCP)

To estimate the moisture content and dry density of the compacted soil layers, the following spot tests were implemented:

- Nuclear Density Gauge (NDG) as per ASTM D6938
- Extraction of compacted geomaterial samples for estimation of oven dry test (as per ASTM D2216)

3.2 IC DATA COLLECTION

At each construction site, the contractor's routine compaction process was followed by a proof mapping. The goal of the proof mapping (a.k.a., final coverage) was to evaluate the compaction uniformity through the identification of less stiff spots and ensuring the complete coverage of the compacted section. Further analyses of the collected IC data during the proof mapping were carried out as further discussed in Chapter 5.

To evaluate the vibration characteristics of the IC systems, a data acquisition system developed by The University of Texas at El Paso (UTEP) research team was also employed. A

schematic of the UTEP's system is shown in Figure 3.2.1 (Nazarian et al, 2015). The system consisted of one or two accelerometers mounted inside the drums to capture the vibration of the drum, a data acquisition system, a GPS antenna/receiver, a power supply and a laptop computer to monitor the data collection process.

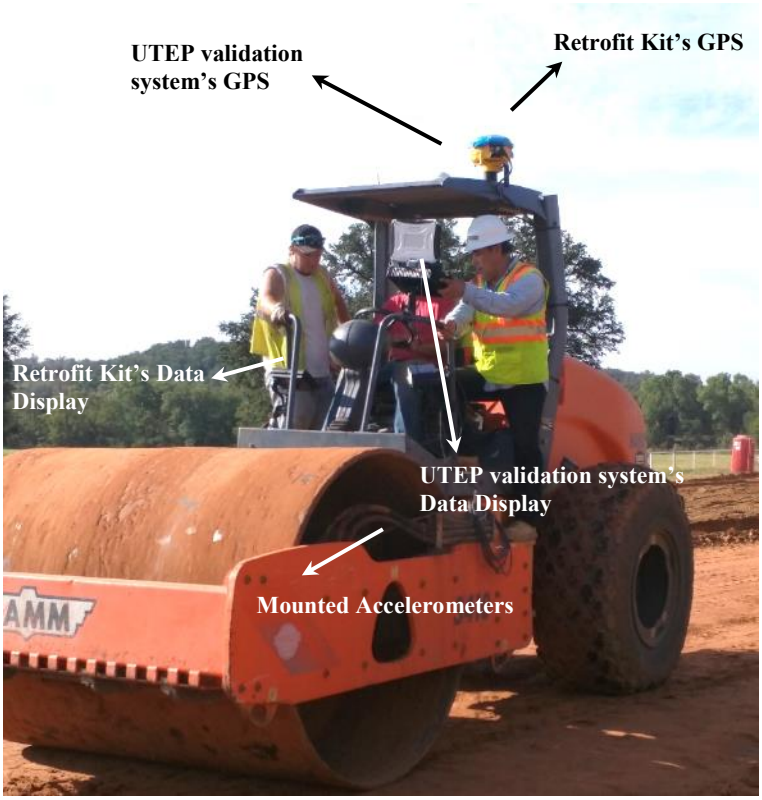

Figure 3.2.1: Schematic of UTEP IC Validation System.

Figure 3.2.2 illustrates the mounted accelerometer for validation purposes as well as the existing IC accelerometer that could be either a part of an OEM system or an IC retrofit kit.

Figure 3.2.2: Mounted Accelerometers from IC Retrofit Kit and UTEP Validation System

Figure 3.2.3 illustrates typical vibration data from mounted accelerometers during data collection. The collected vibration data from the UTEP system in the time domain were converted to the frequency domain using a Fast-Fourier Transform (FFT) algorithm to obtain the roller vibration parameters such as the vibration frequency and its amplitude. In some occasions during this project, the research team installed two accelerometers inside the drum to capture additional vibration data.

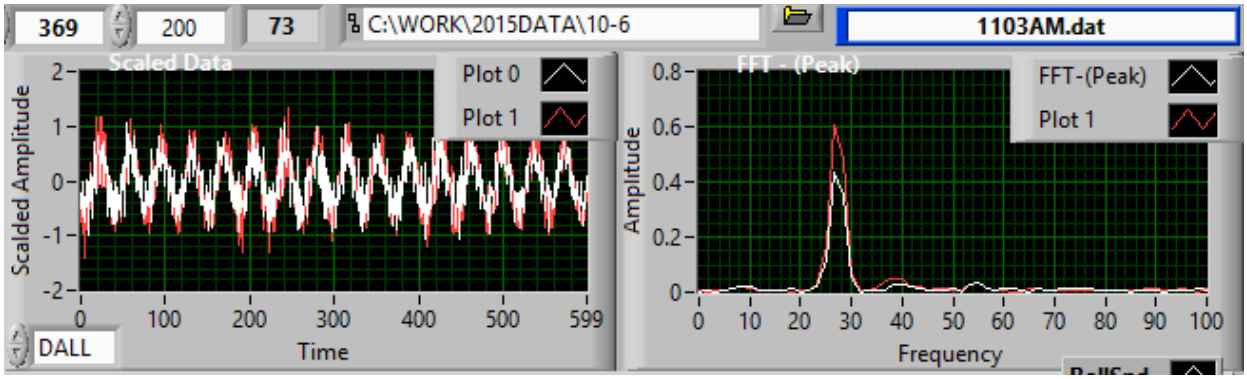

Figure 3.2.3: Typical vibration data collected by UTEP mounted accelerometers (Nazarian et al, 2015)

The intelligent compaction measured value (ICMV) parameter could be regenerated from the frequency-domain vibration data. The calculated ICMVs were then compared to the ICMVs collected by the retrofit/OEM IC system to validate the results of the IC systems. Figure 3.2.4 shows the application of peak frequency and first harmonic frequency (A_2 and A_4 in Figure 3.2.4) to calculate the compaction meter value (CMV) advocated by Caterpillar.

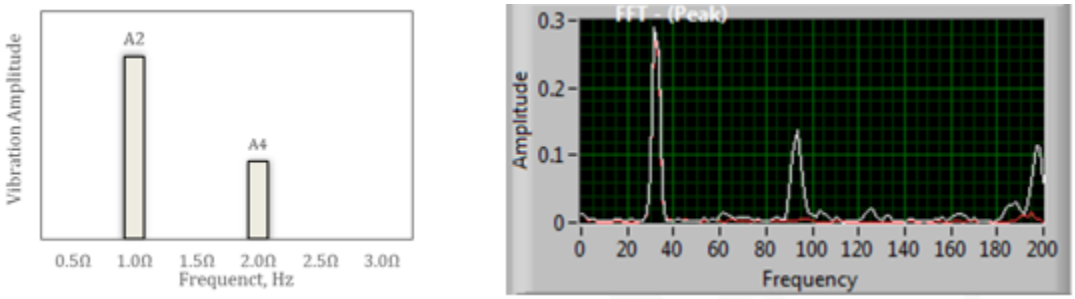

Figure 3.2.4: Extraction of vibration frequency data to calculate CMV (Nazarian et al, 2015)

3.3 GPS CALIBRATION PROCESS

Since a GPS receiver is usually installed on the roller cabin, an offset to the collected GPS position is necessary to adjust the coordinate for the center of the drum. To meet the survey grade precision, the GPS readings from the OEM and retrofit systems need to be calibrated with signals from a land-based GPS base station or virtual reference stations. The process of GPS calibration is shown in Figure 3.3.1 and Figure 3.3.2. The IC roller moves slowly to a designated position to allow the system to stabilize. Once the roller's position becomes static, the GPS coordinates reading, which is associated with the center of the drum, is recorded. The coordinates of both sides of the drum (Figure 3.3.2) are then recorded using a handheld survey-grade GPS rover that was previously synched with the local base station (Figure 3.3.1). The coordinates of the drum center could be interpolated from the coordinates of the two sides of the drum. The coordinates reported by the OEM/retrofit IC system are then compared with the

Figure 3.3.1: Mapping test section using local base station.

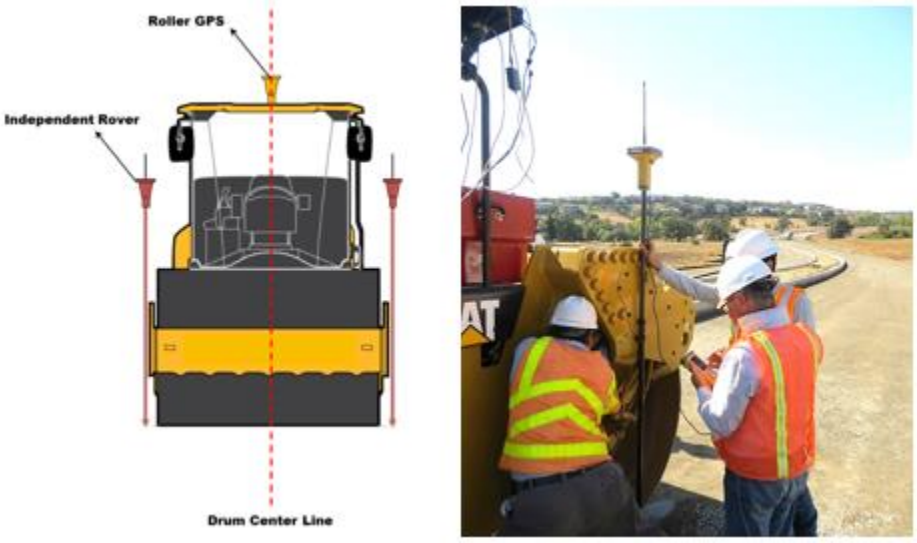

Figure 3.3.2: GPS calibration process (Nazarian et al, 2015)

coordinates interpolated using the coordinates from handheld rover. If necessary, the OEM/ retrofit systems' coordinates are transformed to match the estimated coordinate system. The tolerance of the differences is typically 12 in. in the northing and easting directions, as recommended in the FHWA generic IC specifications. Such validation process is strongly recommended before starting the IC data collection process to avoid the data shifts or erroneous setup.

The Universal Transverse Mercator (UTM) coordinate system was typically used to locate and map the test section. The GPS systems on the IC rollers could either use a local or virtual base station. The Virtual Reference System (VRS) in Texas is usually used to calibrate the IC GPS systems when a local base station is not available at the construction site. The VRS connection sometimes generated some difficulties prior to the initiation of the IC data collection. Such concerns will be discussed in Chapter 5.

3.4 IC DATA MANAGEMENT

Most of the IC system vendors provide an online data management tool to save and manage the collected IC data during a construction process. However, these data management tools provide the user with the option to export the IC data in comma separated variables (csv) format for further analysis. Table 3.4.1 summarizes the data management tools and file formats for three IC vendors. The Trimble® and Topcon® IC retrofit kits support the same file formats as in Table 3.4.1. Since most of the IC rollers employed in this project used the Trimble® system, either as the retrofit kit or as the OEM system on the CAT rollers, the Visionlink® online data management tool was employed to extract and export the collected IC data. For each project, a unique username and password was assigned to the TxDOT engineer and the research team to access the site-specific IC data.

Table 3.4.1: IC data formats and management tools

Roller Vendor	HAMM	CAT and Trimble	SAKAI
Native Data Format	*.hcqx	*.tag	*.ml3
Exported Gridded Data Format	*_amd.vexp, *_pmd.vexp	*.csv	*.pln and *.plns
Software	HCQ	VisionLink®	TOPCON SiteLink3D

3.5 GEOSPATIAL ANALYSIS OF IC DATA

Geostatistical and geospatial data analysis techniques were employed to visualize and interpret the IC data. The two common tools for the visualization of the IC data and performing additional analyses are Veta® and ArcGIS. Each tool has its own advantages and its limitations. Veta is user-friendly and is required as a standard tool in the FHWA, AASHTO, and many State DOT's specifications. ArcGIS provides more flexibility for rigorous analyses and visualization to expert users. Both tools were employed in this project to represent the collected IC data. The IC data were exported from the vendors' data management tool to a "csv" file. The processes of the IC data analyses with each software are briefly summarized in the following steps:

- Import .csv data file into the software environment
- Display the IC data on the map based on the coordinate system used during data collection. The UTM system employs Northing and Easting coordinates to locate the data points. The geographical coordinate system uses Latitude and Longitude data. Both UTM and geographical coordinate systems are used to collect and analyze IC data in this project
- Identify the boundaries to select the desired test section from the total covered area and filter the IC data within the boundary limits
- Perform geostatistical analyses on the collected IC data to generate customized color-coded maps and reports.

Chapter 4: IC Implementation in Paris, Texas

The main purpose of this chapter is to summarize the analysis performed during construction of a test section on highway SH24. This chapter describes the spatial distribution and the possible correlation between the IC retrofit data and NDTs.

4.1 PARIS DISTRICT, STATE HIGHWAY (SH) 24

This test section was a part of the expansion of SH24 near Cooper, Texas in Paris District. The research team assisted the project staff and the contractor representatives from August 12, 2015 to September 18, 2015. This observation involved a number of field visits by the research team.

Figure 4.1.1a shows an aerial view of the location of test section alongside with the stationing map. This figure also illustrates the location of test grid where spot tests were performed by the research team.

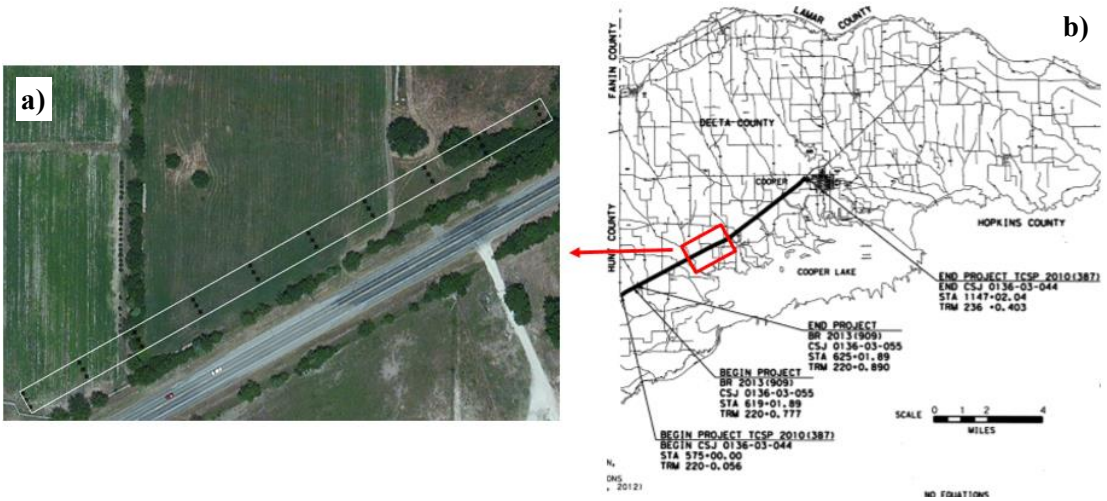

Figure 4.1.1: a) Aerial view and b) Stationing map of the test section along state highway SH24

Lime Treated Subgrade

The existing subgrade layer was pre-mapped using a pad-foot CAT roller equipped with a Trimble® IC retrofit kit. The first phase of the construction work was involved with stabilizing the subgrade soil using hydrated lime. The designed thickness of the lime treated subgrade (LTS) layer was 8 in. The LTS layer was placed, compacted, and mapped using the IC roller on August 12, 2015.

Figures 4.1.2 and 4.1.3 illustrate the spatial distributions of the CMVs collected using the pad-foot roller during the pre-mapping of the existing layer and mapping of the LTS layer, respectively. The location of the less stiff areas on both maps are comparable. The histograms of the pre-mapped and mapped CMVs are summarized in Figures 4.1.4 and 4.1.5. The norms of the CMVs are around 10 for both the pre-mapped and mapped layers. The coefficients of variation (COVs) of the collected CMVs are around 48% for the LTS layer and 49% for the existing layer.

Once the compaction and mapping of the lime-treated subgrade completed, the spot tests with the LWD, DCP and NDG were performed on the compacted layer. A total of 30 spot tests per device were conducted within the test section (see Figure 3.1.1). The collected spot test data were imported into the ArcGIS software to generate the color-coded geospatial distribution maps. The Empirical Bayesian Kriging spatial interpolation algorithm was employed in this process. The advantage of this method as compared to the classical Kriging is that it uses semivariograms estimated from the actual data followed by generation of simulated data from the initial semivariograms. A new semivariogram model is then generated from the simulated data.

Figure 4.1.2: Spatial distribution of CMV data collected by IC retrofit system during pre-mapping of existing subgrade layer

Figure 4.1.3: Spatial distribution of CMV data collected by IC retrofit system during mapping of compacted LTS layer

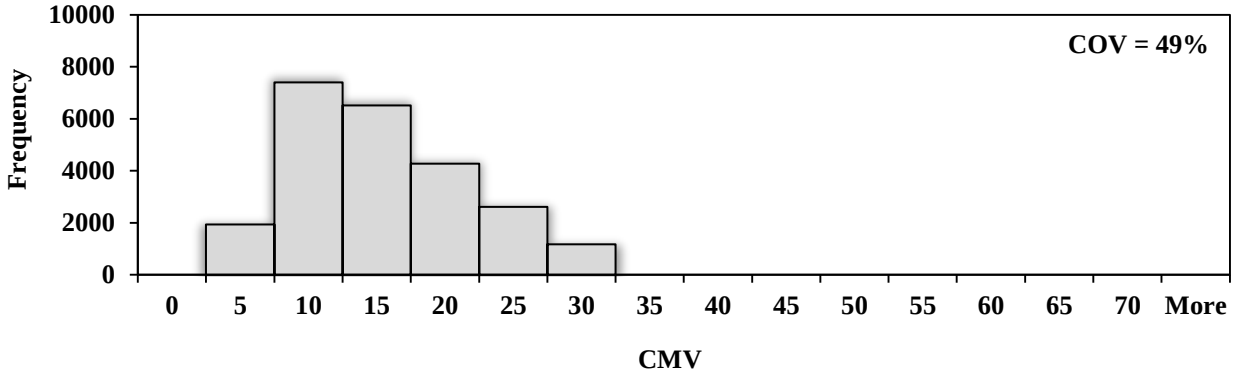

Figure 4.1.4: Distribution of CMV data during pre-mapping of existing subgrade Layer

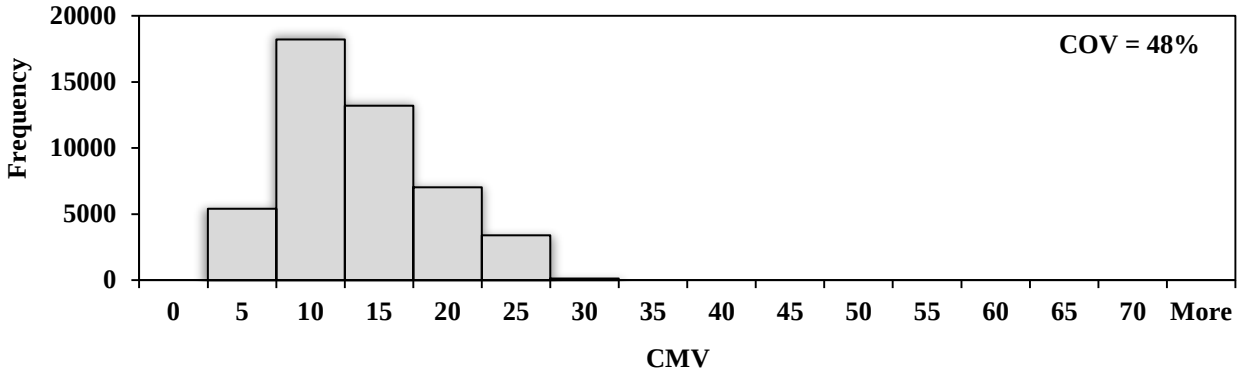

Figure 4.1.5: Distribution of CMV data during mapping of lime treated subgrade Layer

The weight of the latest semivariogram is estimated using the Bayes rule which indicates the likelihood of the observed data being generated from the semivariogram model (Gribov and Krivoruchko, 2012). The Quantile Classification method was employed to classify the data into three colors. This method distributes a set of values into groups that contain the equal numbers of values.

In order to correlate the IC data with the different spot tests, a buffer for all three layers LTS, CTB and FB of 3 ft in radius for every spot test was made. All IC measurements within the three feet radius were averaged and correlated for every spot test. Figure 4.1.6 shows the correlation between CMV and LWD modulus after the compaction of the LTS layer. Appendix A.1 includes detailed information of the regression analyses between the IC data and the other spot

tests collected during the construction on of LTS layer. Since the influence depth for the IC roller and the LWD are different, no strong correlation between the LWD and IC data was found. Strong correlations between the results from the IC roller and the other NDT devices, i.e. DCP and NDG, were not found.

Figure 4.1.7 illustrates the spatial distribution of the LWD modulus on top of the compacted LTS layer. The LWD moduli varied from 1 ksi to 14 ksi with an average of 8 ksi and a COV of 45%. The northeastern part of the test section showed lower LWD moduli which is in agreement with the CMV data in Figures 4.1.2 and 4.1.3.

Figure 4.1.8 summarizes the DCP results on the compacted LTS layer. The estimated DCP moduli ranged from 6 ksi to 25 ksi with an average of 14 ksi and a COV of 31%. The same less-stiff area is recognizable in this figure as compared to the LWD and CMV data. The DCP is a layer specific device since it reflects the properties of the layer of interest as compared to LWD that reports a composite modulus of the underlying layers (Nazarian et al, 2014).

The NDG moisture content and dry density variations are depicted in Figures 4.1.9 and 4.1.10. The LWD and DCP identified the same less stiff area as the IC roller located on the northeast of the test section, while the NDG dry density identified another less stiff area located in the middle of the test section. The color coded maps illustrate a strong spatial correlation between the LWD and DCP. Nevertheless no solid regression analyses between the results from the NDT devices and the ICMVs was found.

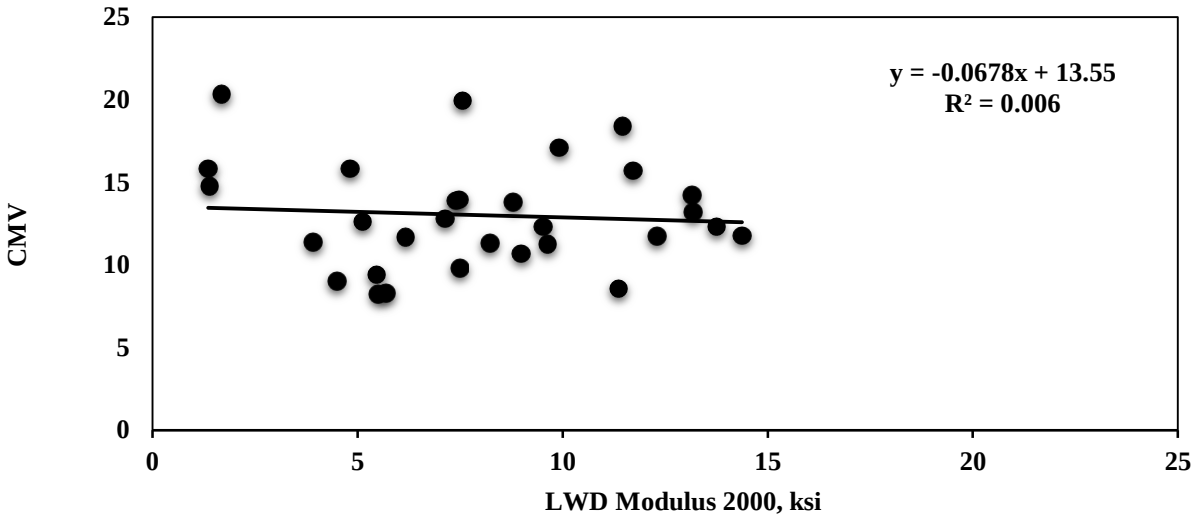

Figure 4.1.6: Correlation between CMV and LWD (model 2000) on compacted LTS layer

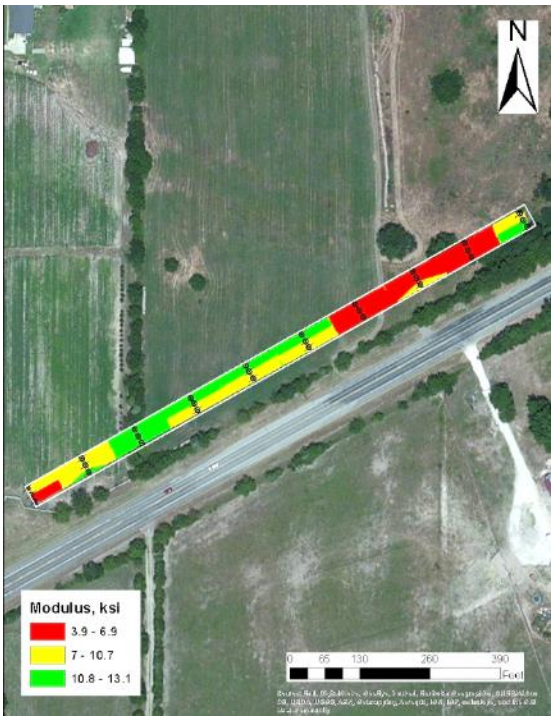

Figure 4.1.7: Spatial variation of LWD (model 2000) moduli on compacted LTS layer

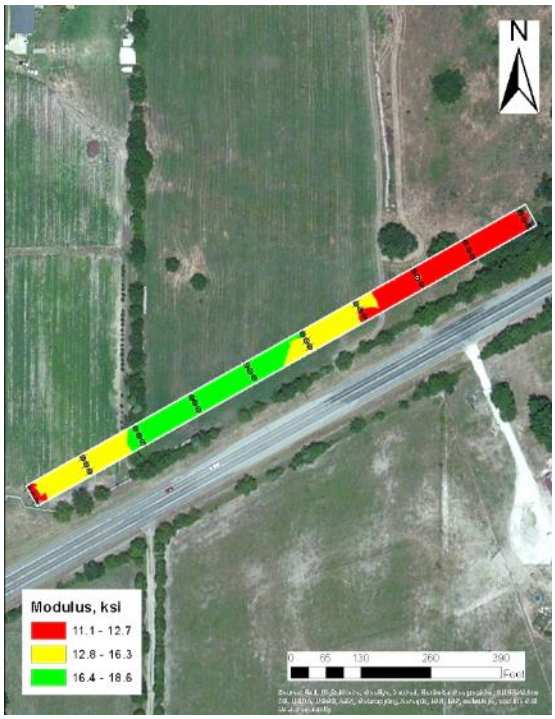

Figure 4.1.8: Spatial variation of DCP moduli on compacted LTS layer

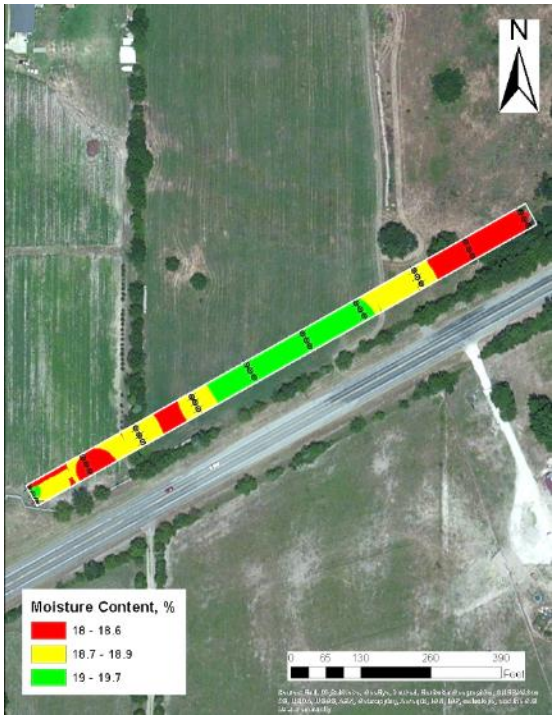

Figure 4.1.9: Spatial variation of NDG moisture content on compacted LTS layer

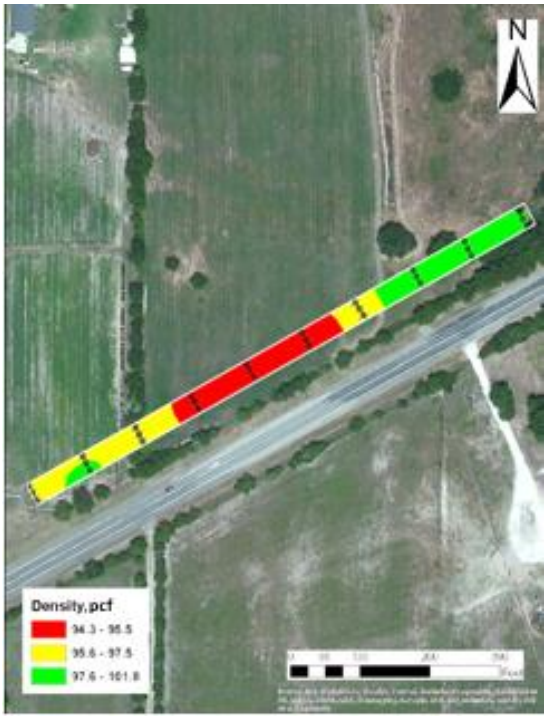

Figure 4.1.10: Spatial variation of NDG dry density on compacted LTS layer

Cement Treated Base

The next construction phase consisted of stabilizing the base materials with cement. The nominal thickness of the cement-treated base (CTB) layer was 8 in. The CTB layer was placed, compacted and mapped using the padfoot IC roller on September 3 and 4, 2015. Due to construction constraints, a small portion of the designated test section was not covered with the CTB layer, and consequently, 27 spot tests were conducted in this phase.

Figure 4.1.11 illustrates the spatial distribution of the CMV data during the mapping of the compacted CTB layer. The blank area in the southwestern end of the test section corresponds to the area that was not covered with CTB. Compared to the CMV data collected on the existing subgrade and LTS in Figures 4.1.2 and 4.1.3, the same less-stiff area could be recognized after mapping the compacted CTB layer.

Figure 4.1.11: Spatial distribution of CMV Data from IC retrofit system during mapping of compacted CTB layer

The histogram of the collected CMV data on the CTB is depicted in Figure 4.1.12. The average CMV is greater than the LTS and existing subgrade layers (see Figures 4.1.4 and 4.1.5) reflecting the higher stiffness of CTB. The COV of the collected CMV data is reduced to 34% for the CTB which represents a more uniform pavement cross section.

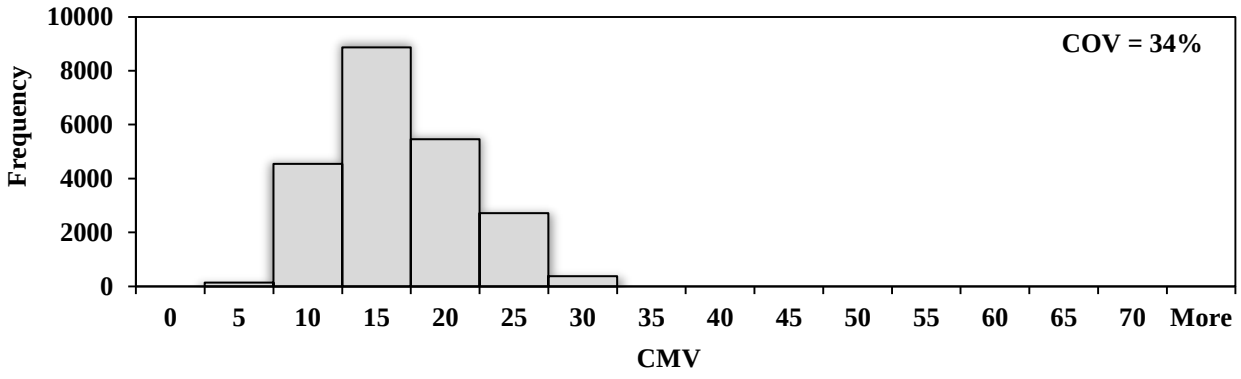

Figure 4.1.12: Distribution of CMV data during mapping of compacted CTB layer

Once the mapping process was complete, the spot tests were conducted on top of the compacted CTB. Figure 4.1.13 shows the correlation between CMV and LWD after the

compaction of the CTB layer. Similar to the LTS layer, since the influence depth for the IC roller and the LWD are different, a strong correlation between the LWD and IC data was not found. Appendix A.2 includes detailed information of the regression analysis between IC data and spot tests collected during the construction of the CTB layer.

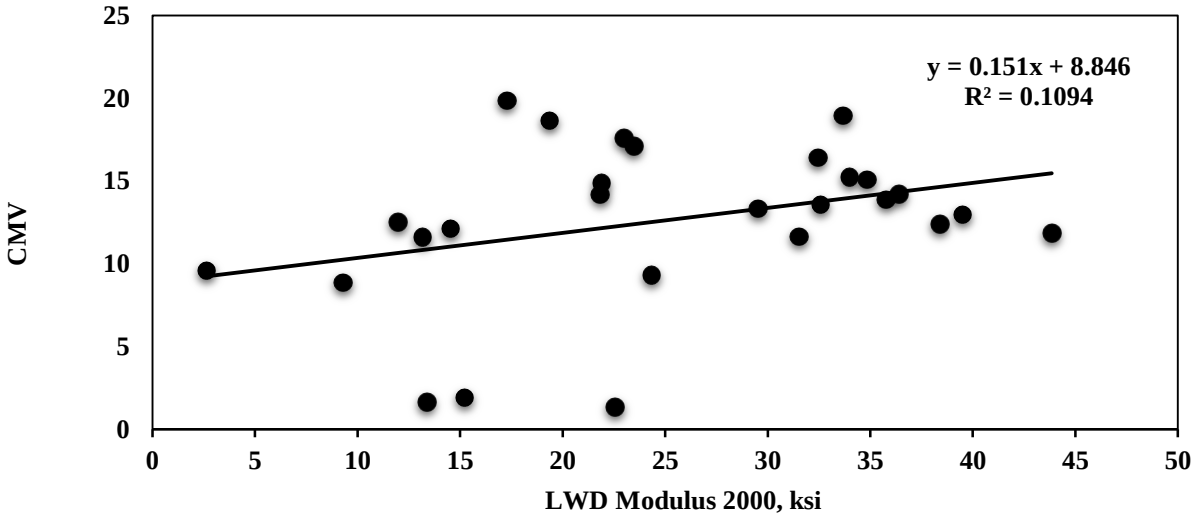

Figure 4.1.13: Correlation between CMV and LWD modulus (model 2000) on compacted CTB layer

The LWD moduli varied from 4 ksi to 48 ksi with an average of 29 ksi and COV of 44% (see Figure 4.1.14). Due to extreme rigidity of the CTB materials, the DCP and NDG tests were conducted only at a few spots within the test section. Since the collected data was not sufficient to generate the color-coded spatial distribution maps, an FWD was employed to perform the spot tests. Figure 4.1.15 summarizes the spatial distribution of the FWD moduli. The estimated FWD moduli varied from 25 ksi to 693 ksi with an average of 261 ksi and COV of 79%. The LWD modulus results did not reflect a clear correlation with the CMV data, as shown in Figure 4.1.11. Nevertheless, the FWD modulus data showed more comparable results to CMV in terms of the identification of the less-stiff areas.

Figure 4.1.14: Spatial variation of LWD (model 2000) moduli on compacted CTB Layer

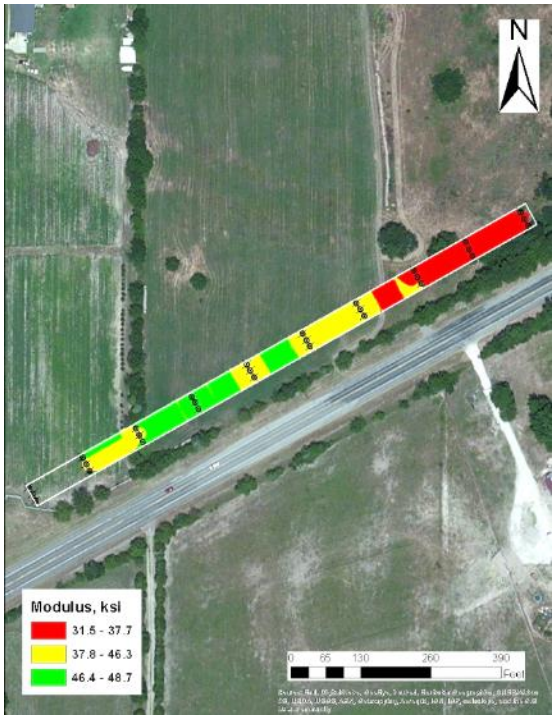

Figure 4.1.15: Spatial variation of FWD moduli on compacted CTB Layer

Flexible Base

The last phase of the construction consisted of placing and compacting untreated (flexible) base materials. The design thickness of the flexible base (FB) layer was 6 in. The area mapped and tested with the CTB was also mapped and tested for the FB materials.

Figure 4.1.16 illustrates the spatial distribution of the CMV data during the mapping of the compacted FB layer. There is a noticeable change in the location of the less-stiff areas in this layer as compared to previous layers. Likewise, the histogram of the CMV distribution depicted in Figure 4.1.17 exhibits a considerable change in the trend of the collected CMV data. The average CMV of 41 seems to be greater than the previous CTB layers and the COV is reduced to 27%. This change in the pattern of the collected CMVs is mostly due to the influence depth of the IC roller and the fact that CMV is an estimation of a composite stiffness of several layers.

Figure 4.1.16: Spatial distribution of CMV Data from IC retrofit system during mapping of compacted FB layer

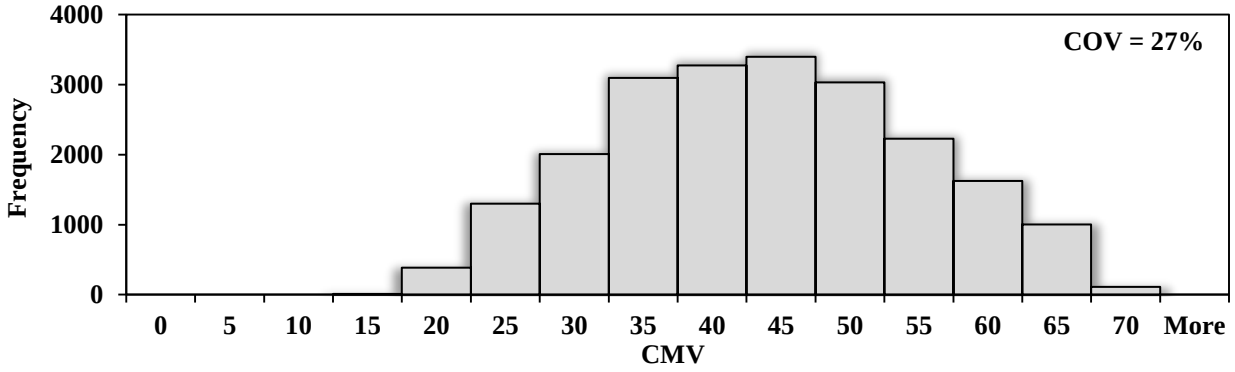

Figure 4.1.17: Distribution of CMV data during mapping of compacted FB layer

Figure 4.1.18 compares the cumulative distribution of CMV from the retrofit system collected during the mapping of each lift. There is a manifest increase in the CMV values as the stiffer layers are placed.

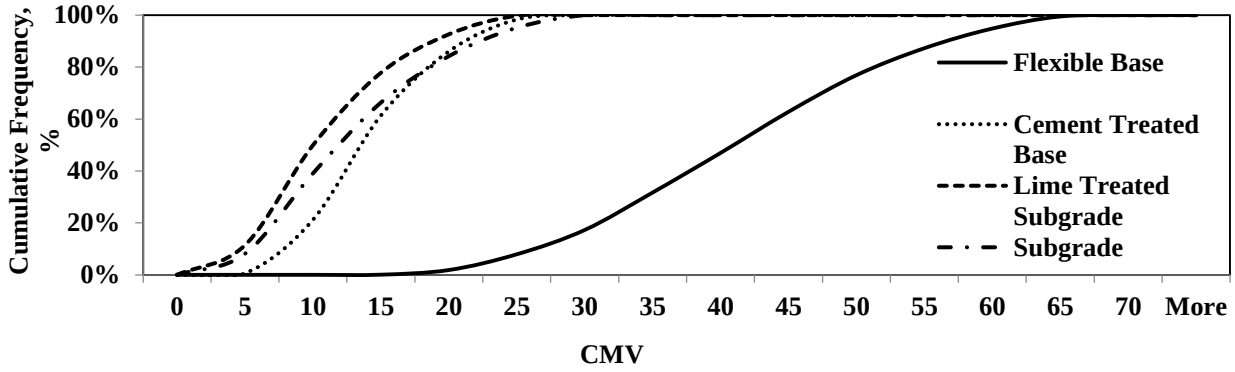

Figure 4.1.18: Comparison of CMV values during mapping of each layer

Figure 4.1.19 shows the correlation between CMV and LWD after the compaction of the FB layer. Appendix A.3 includes detailed information of the regression analysis between the IC data and the results from the spot tests collected during the construction on of FB layer. Again, since the influence depth for the IC roller and the LWD are different, no solid correlation between the LWD and IC data was found..

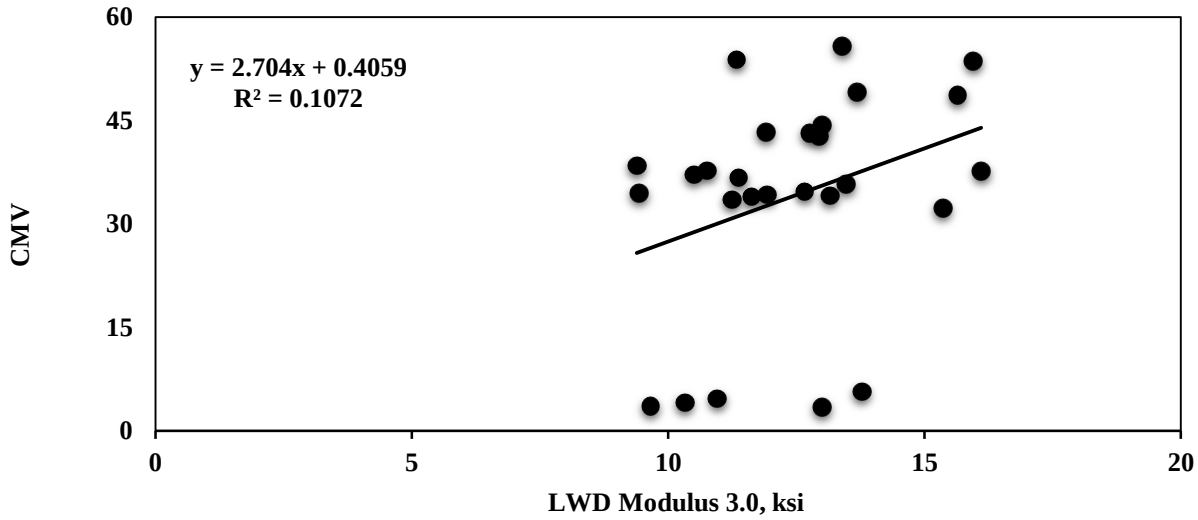

Figure 4.1.19: Correlation between CMV and LWD (model 3.0) on compacted FB layer

A spatial analysis was conducted for LWD and FWD within the test section. The LWD moduli vary from 9 ksi to 16 ksi, with an average of 12 ksi and COV of 15% (see Figure 4.1.20). Figure 4.1.21 summarizes the spatial distribution of the FWD data. The FWD moduli changed from 22 ksi to 55 ksi, with an average of 38 ksi and COV of 21%. Again, since DCP and NDG tests were only feasible on few locations, their distribution maps are not available. Comparing the LWD and FWD results with the collected CMV data during the mapping of the FB layers, there is a noticeable similarity between the trend of interpolated spot test data and CMV results in terms of identification of less stiff spots. The FWD shows an evident spatial correlation with the IC data. The LWD does not reveal a strong correlation neither for regression analysis nor spatial distribution with IC data.

Figure 4.1.20: Spatial variation of LWD (model 3.0) moduli on compacted FB layer

Figure 4.1.21: Spatial variation of FWD moduli on compacted FB layer

Chapter 5: Evaluation of IC Data in Cleburne, Texas

The objective of this chapter was to evaluate the change in CMV between passes using the data from Cleburne, Texas. As discussed in Section 3.2, vibration data was recorded using a validation system that was developed for the IC data collection that resembles the retrofit systems (Nazarian et al, 2015). For this study, the validation system was tested and mounted on two rollers (HAMM and SAKAI) for a duration of two days (November 18 and 19, 2015). Section 5.2 summarizes the results during the first day of testing using the reduced sensor data from the mounted accelerometers on the rollers. The detailed analyses for the first and second day of data collected with the UTEP validation system are included in Appendix B.

5.1 INTRODUCTION

The study was performed on a 500 ft long and 24 ft wide test section on the eastbound frontage road as part of the expansion of the US 67 Business and County Road 801B near Cleburne, Texas (Figure 5.1.1). For this project, the existing embankment layer was compacted and mapped during the first day using the three rollers (CAT, SAKAI and HAMM) equipped with both the retrofit kit and the UTEP validation system. The clayey subgrade layer (12 in.) was placed and compacted on the second day of operation and then mapped with the same three IC rollers.

A vibration analysis was also performed along an 80-ft-long stretch within the test section in order to evaluate the ICMV between passes. To evaluate every roller pass the test section was divided into three lanes A, B, and C (Figure 5.1.2). All rollers performed several passes on each lane. “One pass” was defined as a one way oriented lane (forward or reverse). However, for simplification purposes only data from lane B was analyzed.

Figure 5.1.1: Location of test section in Cleburne, Texas

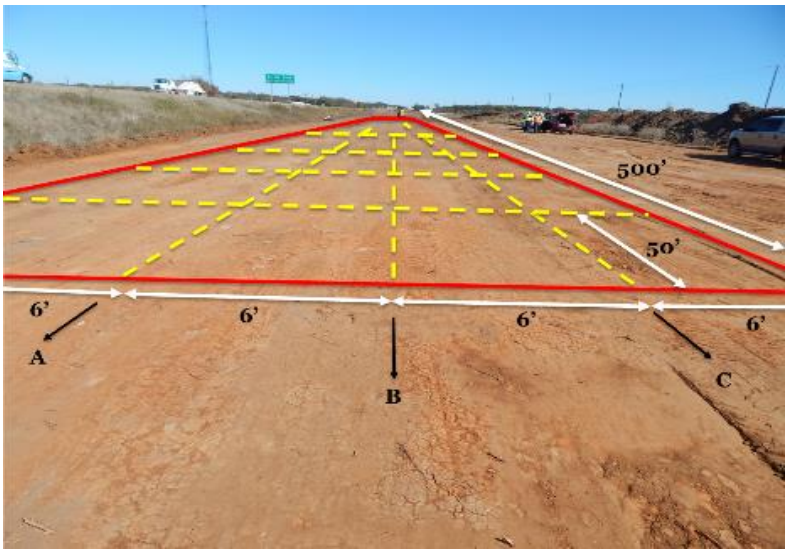

Figure 5.1.2: Test section and grid in Cleburne, Texas

The vibration data were collected from the accelerometers mounted on the rollers. Two geophones were embedded in the ground to measure the soil responses for every pass. The geophone is only used as a reference point in the vibration analysis. Figure 5.1.3 shows the location of one of the SAKAI roller passes during the pre-mapping process with respect to the location of the embedded geophones and the boundaries of the test section.

Figure 5.1.3: Location of roller pass with respect to geophone locations and tests section in Texas

During the compaction process, an area equal to the width of the drum is covered in each pass and gridded with the retrofit kit. The gridded area is then compared with the measured GPS locations provided by the validation system as shown in Figure 5.1.4. The vibration frequency and amplitude, as well as the estimated ICMVs, were extended to the width of the roller at each point. The spatial analyses were performed on the gridded data hereafter. Section 5.2 includes the details of the vibration data from the mounted accelerometers followed by their spatial analyses.

Figure 5.1.5 illustrates an example of the frequency spectrum from the accelerometer data during the moving vibration tests. The fundamental frequency and the first harmonic component of the vibration are identifiable in this figure. The acceleration amplitudes at these two frequencies were utilized to estimate the stiffness in terms of the CMV (Eq. 2.3.1).

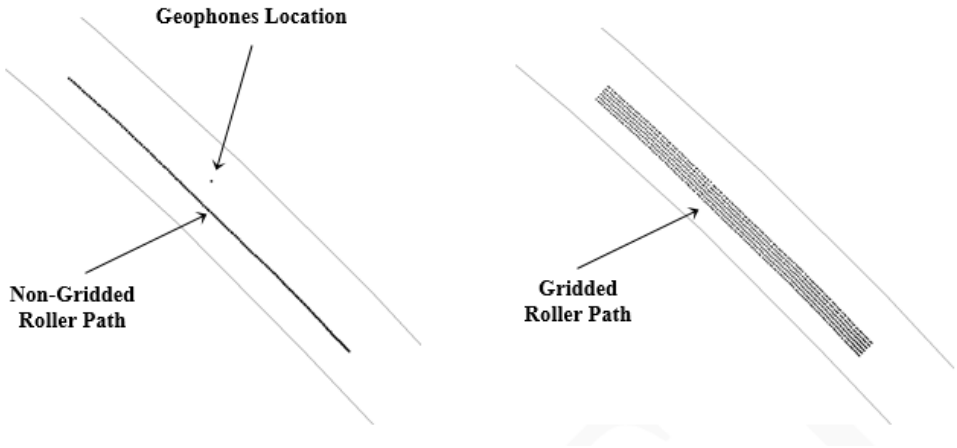

Figure 5.1.4: Gridded data points compared to the original GPS locations (Nazarian et al, 2015)

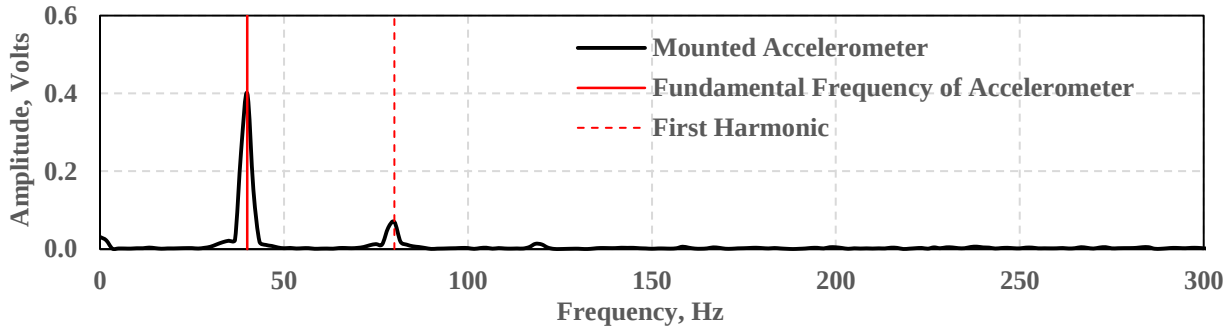

Figure 5.1.5: An example of vibration data from mounted accelerometer

Table 5.1.1 summarizes the specifications of the three single drum rollers employed in the soil compaction process in Cleburne, TX. Each roller manufacturer uses their own parameter for compaction which consist in the following setting:

- Low frequency and low amplitude
- High frequency and low amplitude
- Low frequency and high amplitude
- High frequency and high amplitude

Table 5.1.1: Specification of single drum rollers employed in Cleburne, TX.

Vendor/ Manufacturer	CAT	SAKAI	HAMM
Model	Single-drum IC roller with a padfoot shell kit - CS74B	Single-drum padfoot IC roller (with smooth drum shell kit) - SV540T	HD120 Vibratory Smooth Drum Roller
Amplitude, mm	0.991 – 2.11	0.940 – 1.93	0.838 – 2.03
Frequency, Hz	23 – 28	28 – 33	30 – 40

Figure 5.1.6 demonstrates the ideal results expected in the form of a spectrogram that shows the fundamental frequency and the first harmonic mode of the accelerometer data during compaction with the SAKAI roller. A spectrogram is a graph of the amplitude spectra accumulated at different times during the vibration of the drum. The fundamental frequency of the vibration is shown as the darkest strip in each spectrogram. The y-axis denotes the distance of the roller from the location of the embedded geophones. The negative distances correspond to the data before the roller arrived at the geophone location. The spectrogram shows the fundamental frequency of

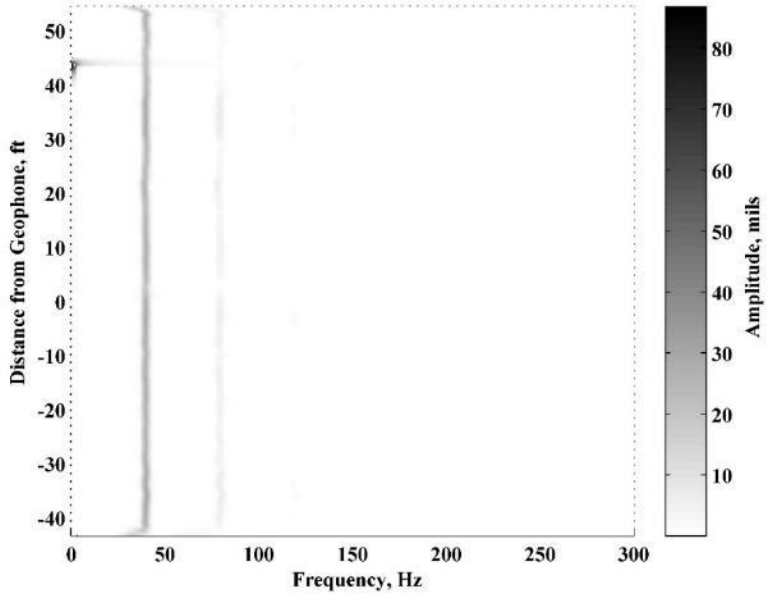

Figure 5.1.6: Spectrogram of vibration data from mounted accelerometer for one roller pass (SAKAI roller)

approximately 40 Hz. The faded areas at the bottom and top of the graph represents the initiation and termination of the roller vibration. Table 5.1.2 describes the pass number, the manufacturer roller used, and the availability for the systems used in every pass.

Table 5.1.2: IC systems available during compaction in Cleburne, Texas.

Pass No.	Manufacturer	Retrofit Kit	UTEP Sensors
First Day (November 18)			
1	HAMM	Available	Available
2	HAMM	Available	Available
3	CAT	Available	N/A
4	CAT	Available	N/A
5	SAKAI	Available	Available
6	SAKAI	Available	Available
Second Day (November 19)			
1	CAT	Available	N/A
2	CAT	Available	N/A
3	CAT	Available	N/A
4	CAT	Available	N/A
5	CAT	Available	N/A
6	CAT	Available	N/A
7	HAMM	Available	N/A
8	HAMM	Available	N/A
9	SAKAI	Available	Available
10	SAKAI	Available	Available
11	SAKAI	Available	Available
12	SAKAI	Available	Available

5.2 VIBRATION EVALUATION OF IC ROLLER DURING FIRST DAY

This section covers the influence of the frequency and amplitude on the CMV readings between roller passes on top of the embankment layer during the first day of compaction. A detailed comparison was performed between pass number 1 and pass number 6 from the different rollers and the UTEP sensors for Lane B. Due to time constraints, the vibration system was only mounted on the SAKAI and HAMM roller. Even though the CAT roller did compact during the

third and fourth pass, the evaluation between the retrofit and UTEP sensors was not feasible. However, a spatial analyses for the data obtained from the retrofit kit installed on the CAT roller was used to create a color coded map.

Figure 5.2.1 depicts that the forcing frequencies from the UTEP system and the retrofit kit installed on the HAMM roller were around 20 Hz. The forcing frequencies from both the UTEP system and the retrofit kit installed on the SAKAI roller are shown in Figure 5.2.2. The forcing frequency for the SAKAI roller was around 32 Hz. In both graphs, the frequencies differ only slightly showing a solid relation between the two systems.

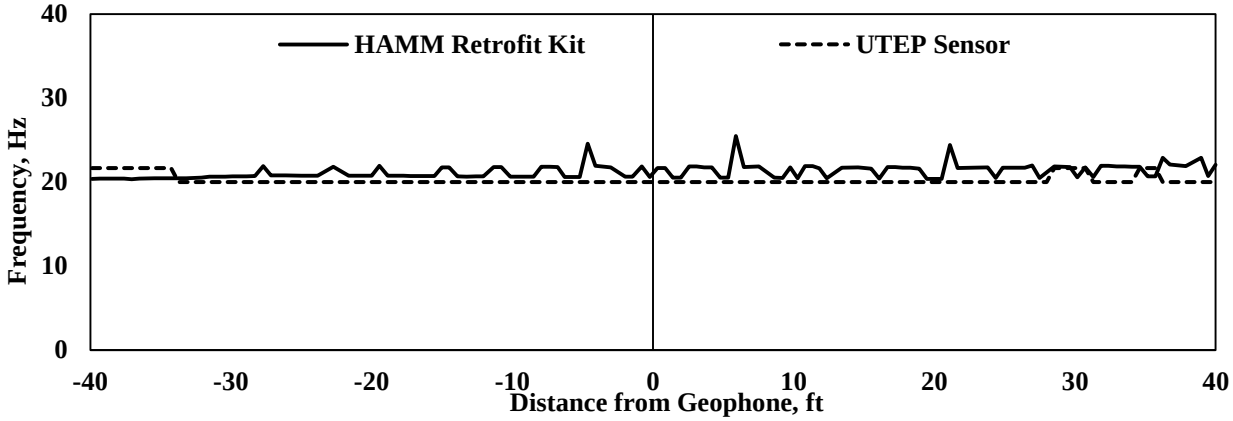

Figure 5.2.1: Comparison of vibration frequency data from validation system with retrofit kit for the first roller pass (HAMM roller)

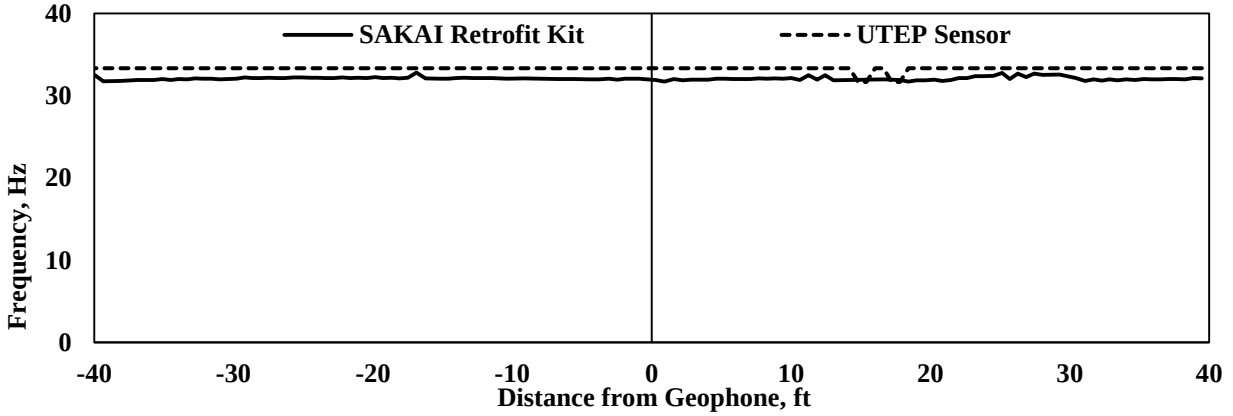

Figure 5.2.2: Comparison of vibration frequency data from validation system with retrofit kit for the sixth roller pass (SAKAI roller)

Figure 5.2.3 illustrates the spectrogram of the vibration of the drum during the first pass of the HAMM roller at a low frequency and a high amplitude. The first harmonic is visible between the fundamental frequency and 50 Hz on the x-axis. Figure 5.2.4 shows the spectrogram for the SAKAI roller during the sixth pass closer to a fundamental frequency of 32 Hz. The first harmonic is not visible. HAMM exhibits better responses illustrated in the spectrogram than SAKAI since the first harmonic appears about twice the fundamental frequency as the CMV definition stated.

The forcing frequency throughout the 80 ft long test section of each pass was averaged. Figure 5.2.5 illustrates the average fundamental frequency from the retrofit kit and the validation system for the HAMM and SAKAI rollers. As previously stated, UTEP sensors were not mounted on the CAT roller which covered the third and fourth passes. The fundamental frequencies for the first, fifth, and sixth passes are the same, except for the frequency of the second pass. For the second pass (HAMM roller), there was a difference of about 8 Hz between the validation system and the retrofit kit. This dissimilarity between the frequencies might have influenced the CMV responses during the second pass.

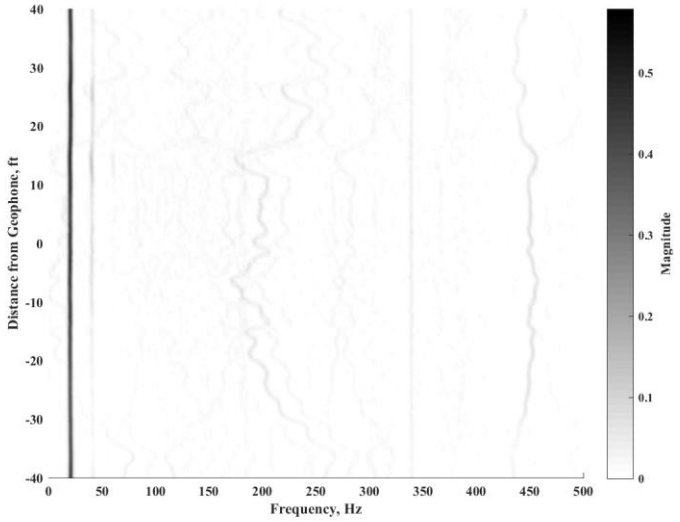

Figure 5.2.3: Spectrogram of vibration data from mounted accelerometer for the first pass on HAMM roller (Nov.18)

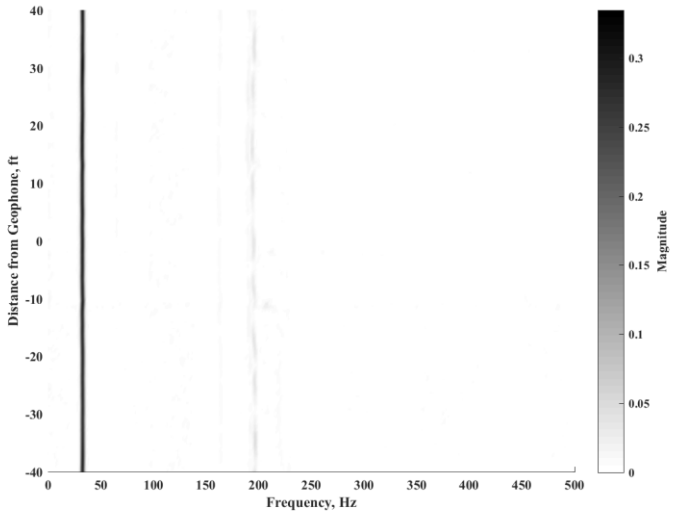

Figure 5.2.4: Spectrogram of vibration data from mounted accelerometer for the sixth pass on SAKAI roller (Nov.18)

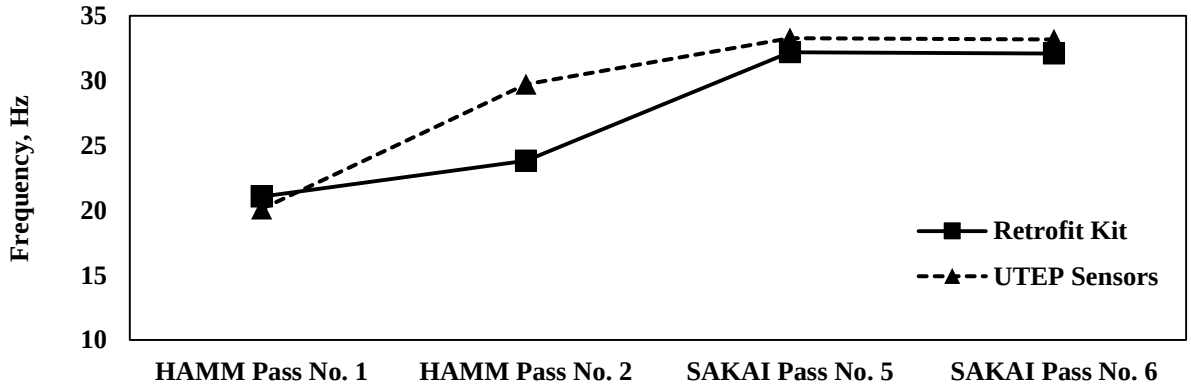

Figure 5.2.5: Comparison of vibration frequency data from retrofit kit and validation system on HAMM and SAKAI rollers between different passes (Nov.18)

The retrofit amplitude throughout the 80 ft long in the test section of each pass was averaged. Figure 5.2.6 represents the average amplitudes measured from the retrofit kit for each roller. The first two data points are the average amplitudes for the first and second pass on the HAMM roller (high amplitude), while the last two points are the average amplitude for the fifth and sixth passes on the SAKAI roller (low amplitude).

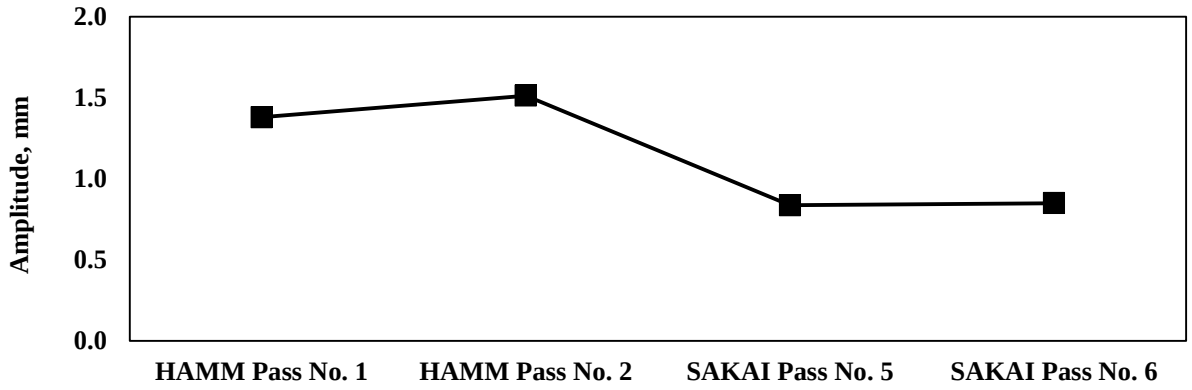

Figure 5.2.6: Comparison of vibration amplitude data from retrofit kit on HAMM and SAKAI rollers between different passes (Nov.18)

The calculated CMVs from the validation system are compared with the reported CMVs by the retrofit kits in Figures 5.2.7 and 5.2.8. The differences can be attributed to the position of the mounted accelerometer on the drum shaft as compared to the position of the retrofit sensor. The data shows that the calculated CMVs are sensitive to the position of the vibration sensor of the UTEP system.

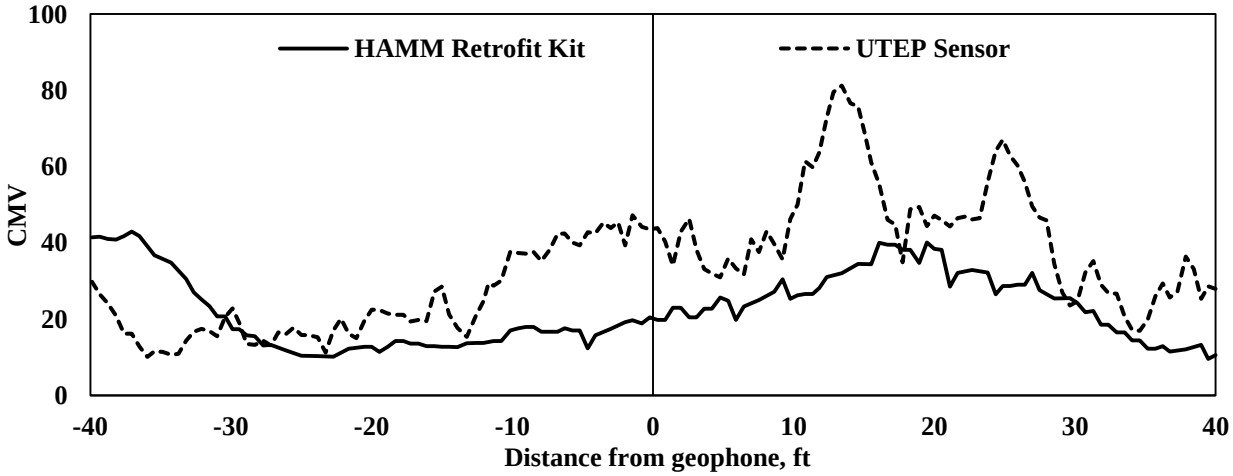

Figure 5.2.7: Comparison of CMV data from validation system and retrofit kit for the first roller pass (HAMM roller)

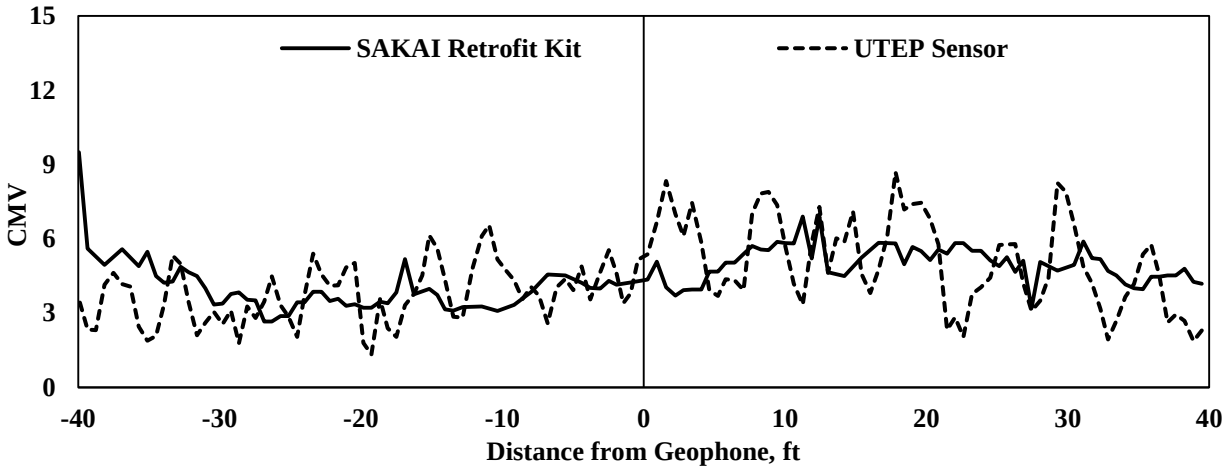

Figure 5.2.8: Comparison of CMV data from validation system and retrofit kit for the sixth roller pass (SAKAI roller)

Figure 5.2.9 compares the cumulative distributions of the CMVs from the UTEP system with the retrofit system on the HAMM roller during the first roller pass. The CMVs from the retrofit system are smaller than those reported from the UTEP system. The slightly dissimilarity of frequencies during the first pass (see Figure 5.2.5) may influence the CMV responses for both systems. On the other hand, the CMV cumulative distribution for both systems, appear to increase at the same rate.

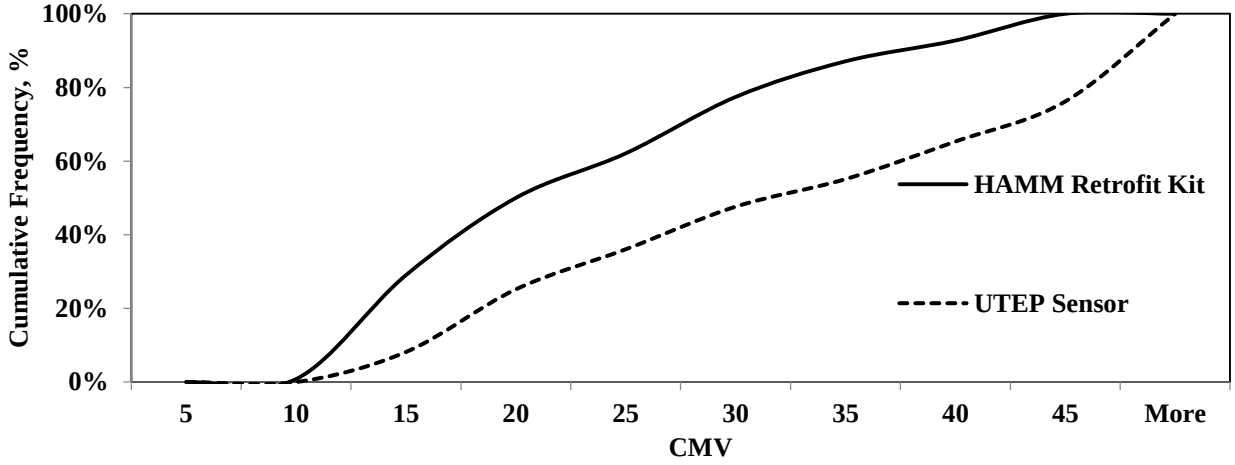

Figure 5.2.9: Comparison of CMV data from validation system and retrofit kit on HAMM roller for the first roller pass

Figure 5.2.10 compares the cumulative distributions of the CMVs from the UTEP system with the retrofit system on the SAKAI roller during the sixth roller pass. Both systems seem to provide similar CMV distributions. The CMVs from the first pass (Figure 5.2.9) that use low frequency and high amplitude are greater than the sixth pass (Figure 5.2.10), which has high frequency and low amplitude. The change in amplitude of the roller vibration seems to have a visible impact on the roller responses.

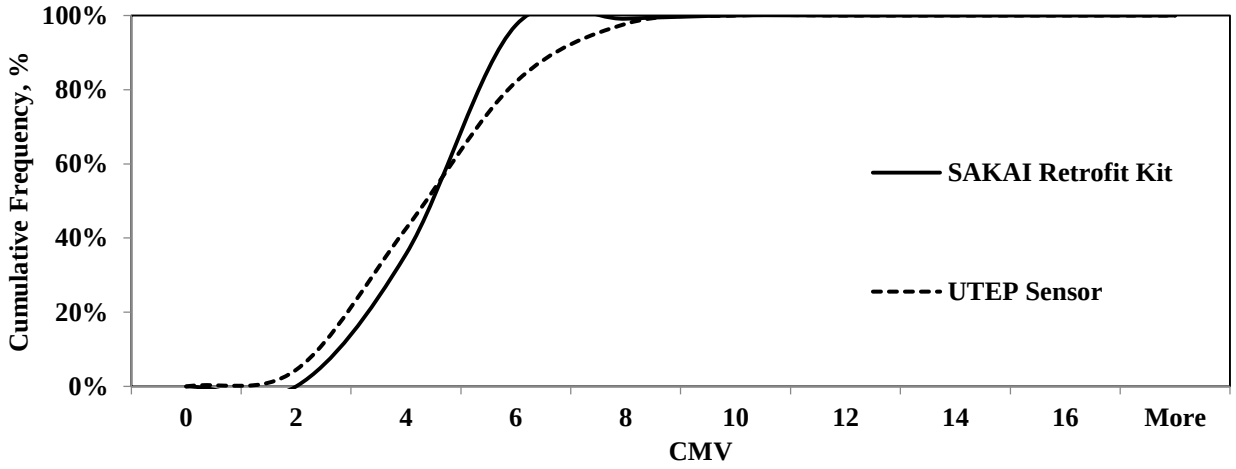

Figure 5.2.10: Comparison of CMV data from validation system and retrofit kit on SAKAI roller for the sixth roller pass

Figure 5.2.11 shows the cumulative distribution of the CMV's from the retrofit kit on the HAMM and SAKAI rollers. The first two passes were collected using the HAMM roller while the third and fourth passes are missing since they were collected with the CAT roller. The last two passes were performed using the SAKAI roller. As seen in Figure 5.2.11, there is a clear distinction between the HAMM and the SAKAI cumulative distributions. A comparison of the cumulative distributions of the CMV's from the UTEP sensors for the HAMM and SAKAI rollers is presented in Figure 5.2.12. Both graphs have similar distributions for all the passes, except for the second pass of the HAMM roller. The difference can be due to the variation in the frequency and amplitude readings for both systems.

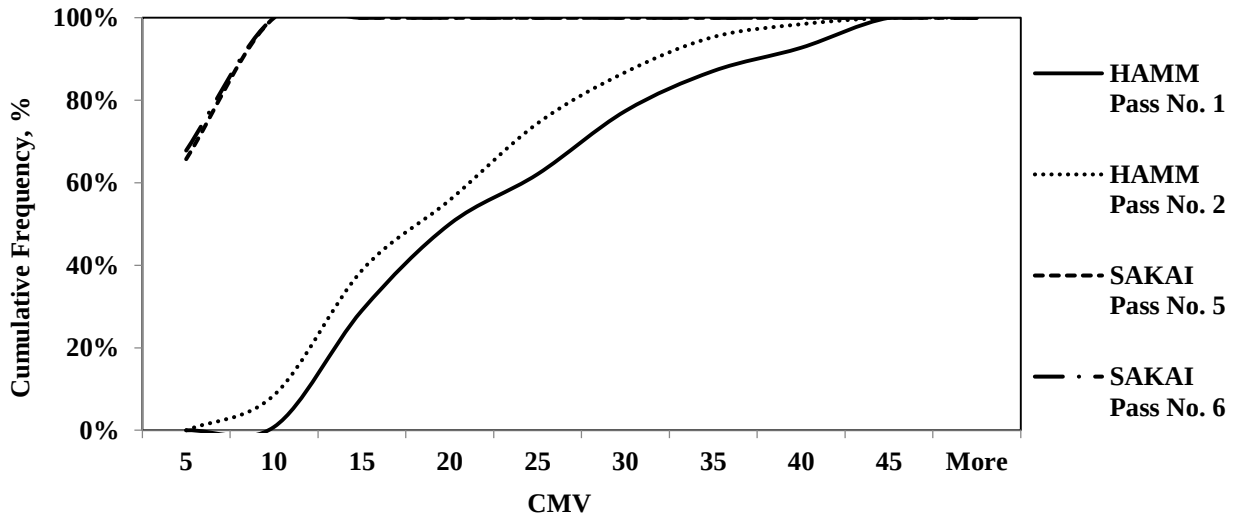

Figure 5.2.11: Comparison of CMV data from retrofit kit on HAMM and SAKAI rollers between different passes (Nov.18)

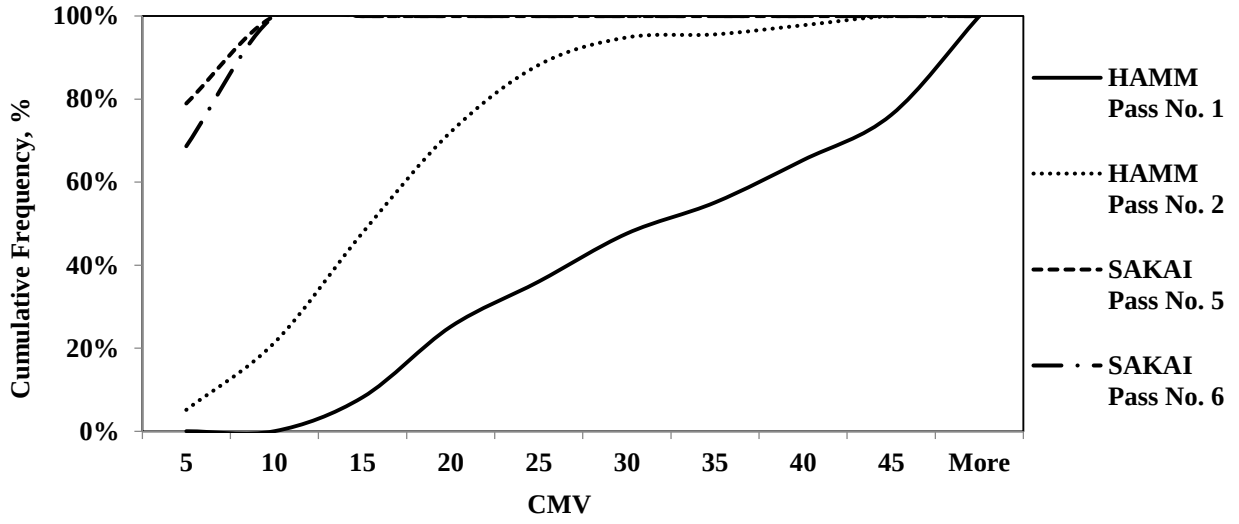

Figure 5.2.12: Comparison of CMV data from validation system on HAMM and SAKAI rollers between different passes (Nov.18)

Figure 5.2.13 compares the cumulative distributions of the CCV's from the UTEP sensors on the HAMM and SAKAI rollers. The HAMM roller, again, shows a higher ICMV distribution than SAKAI roller.

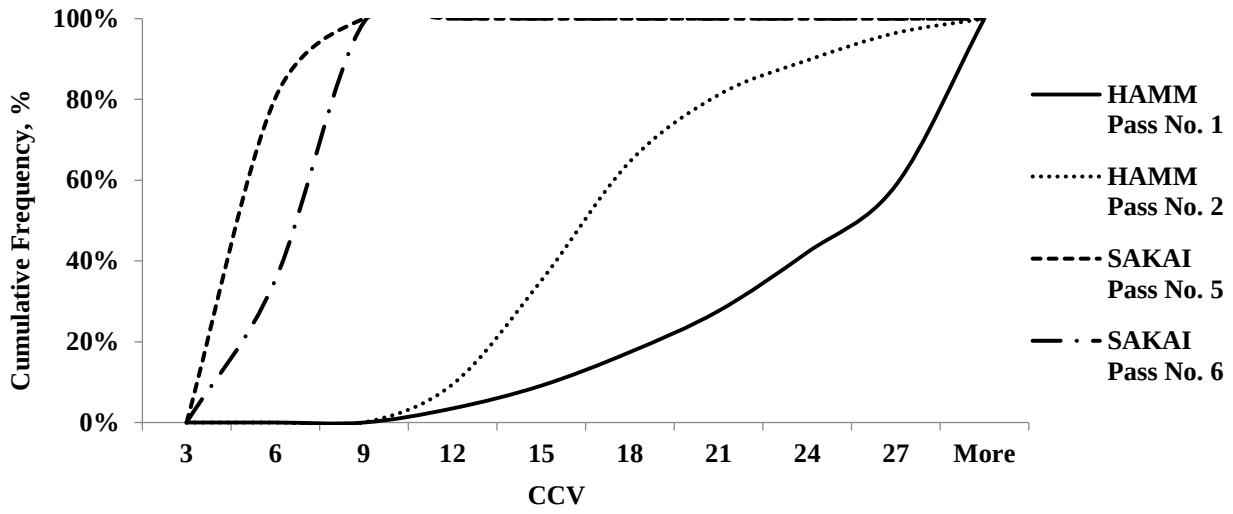

Figure 5.2.13: Comparison of CCV data from validation system on HAMM and SAKAI rollers between different passes (Nov.18)

Figure 5.2.14 illustrates the spatial distributions of the CMVs collected using the HAMM smooth drum roller during the pre-mapping (first pass) of the existing embankment layer. The area at the center of the test section was identified as a less stiff area compared to the rest of the test section. Figure 5.2.15 shows the spatial distributions of the CMVs collected using the CAT pad-foot roller at the last CAT pass (fourth pass) of the existing layer. The smooth drum CAT roller also identified the center area to be the most flexible sections.

Figure 5.2.16 illustrates the spatial distributions of the CMVs collected using the smooth drum roller at the final SAKAI pass (sixth pass) of the existing layer. The location of the less stiff areas in the map are comparable to the previous two rollers. The coefficients of variation (COVs) of the collected CMVs are 42%, 42% and 39%, respectively.

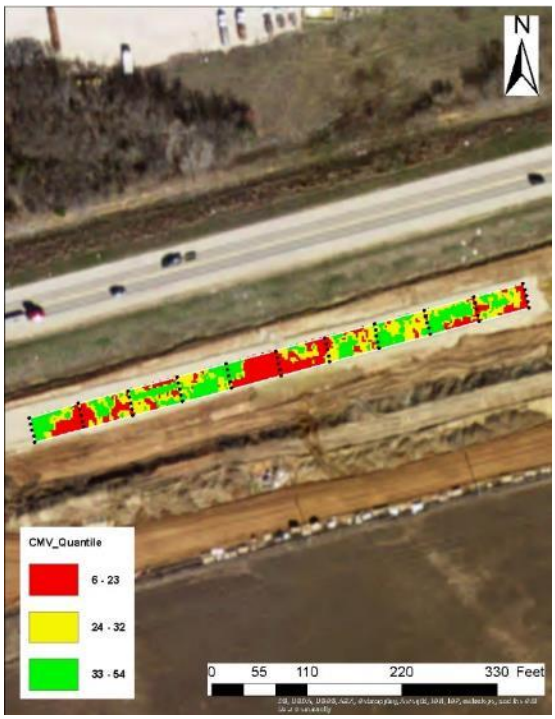

Figure 5.2.14: Spatial distribution of CMV Data from IC retrofit system on HAMM roller after first roller pass

Figure 5.2.15: Spatial distribution of CMV Data from IC retrofit system on CAT roller after fourth roller pass

Figure 5.2.16: Spatial distribution of CMV Data from IC retrofit system on SAKAI roller after sixth roller pass

Chapter 6: Summary and Conclusions

In the state of Texas, the nuclear density gauge is the current practice for field compaction quality control and quality assurance for soil and base layers The target of intelligent compaction is to achieve uniformity in compaction of pavement layers, to improve the quality of construction, and to enhance the performance of pavements with reduced cost of construction. In this research, the use of intelligent compaction was evaluated at two sites on four different materials. The compaction characteristics of two types of subgrade soils, a lime treated subgrade, cement treated base and a flexible base layers were studied. Two different types of roller measurement values and four density and modulus-based NDT devices were used to study the compaction properties of earthwork and unbound aggregates. Upon the completion of two sites investigated and analysis of the collected data from the retrofit kits and UTEP sensors, the following observations and conclusions are presented.

IC Measurement Values and Units: Each IC system estimates the stiffness using a different definition. The retrofit kit provided by Trimble measures the stiffness as Compaction Meter Value (CMV), which is the same as the OEM system on the CAT roller. The vibration data collected with the UTEP Sensors developed for this study are in terms of raw vibration signals that can be used to calculate CMV and CCV.

Geospatial Analysis of IC Data: The findings from the experienced gained during the data analysis from both sites are as follows.

- Shortly after the completion of the IC operation, the collected data should be analyzed as an expedited quality control tool.

- One pragmatic way of almost real time use of the data, given the current complications with setting the target ICMV, is to observe the average ICMV of the last pass which is accessible on the control box of the IC kit. This average value can be used as the reference value to spatially locate relatively soft areas by the contractor.

- The data transfer process was evaluated in this study both using the cloud storage and a thumb drive. Downloading the collected IC data through each vendor's online data management system (e.g., VisionLink for Trimble/CAT, SiteLink3D for Topcon/Sakai and HAMM Compaction Quality navigator) seems to be more straightforward.

- An advanced analysis can be conducted using the ArcGIS package on collected IC data and provides a complete range of coordinate system to locate IC data on different types of geographical and satellite maps while correcting for any possible data offsets. Using this tool requires basic knowledge of ArcGIS and its definitions.

IC Data Analysis and Interpretation: The spatial interpretation of the IC data in terms of color-coded maps is strongly dependent on the classification algorithm employed. The interpretation of color-coded maps also rely on the selected statistical parameters. Since the estimation of the ICMV target values is not very straightforward yet, a standardized statistical method should be employed to interpret the spatial distribution of ICMV data, and furthermore, to identify the under-compacted areas. The standard quantile method was employed in this study to statistically classify the ICMV data and assign three colors (red, green and yellow) to the data points. The generated color-coded maps were then evaluated to identify the weak (soft) spots. In this method, the ICMV data are grouped into three different classes in the way that there are the

same number of data points in each group. This classification method is dependent of the statistical parameters of each set of collected ICMV data and do not require a target ICMV. Classification methods based on defined target ICMV can be defined and standardized in future research efforts. However, utilization of classification based on the mean and standard deviation of ICMV population seems reasonable at this time.

Paris, Tx: The following items were observed during the construction of the layers:

- The IC data collected within the three layers show good trends in the changes in the CMVs as layers are added.
- The CMV "COV" dropped from 48% to 34% to 27% for the Lime Treated Subgrade, Cement Treated Base and Flexible Base.
- Correlations between CMVs with stiffness spot test and density were not very strong which could be due to the influence depth of each device and moisture variation.
- The spatial distributions of CMVs, LWD and FWD moduli were similar as they identified similar less stiff areas.

Cleburne, Tx: The following items were observed during the soils rodeo:

- The ICMV results during the pre-mapping of the existing embankment layer with the retrofit kit mounted on the HAMM roller and the retrofit system on the CAT roller are reasonably similar. The ICMV data collected from the retrofit kit mounted on the SAKAI roller are significantly lower than those reported by the HAMM and CAT retrofit systems. This could be due to unidentified malfunction in transmitting or transferring the associated data collection process.

- The spatial distributions of the CMVs in color-coded maps from mapping the compacted subgrade layer with a retrofit system on HAMM (Smooth drum), CAT (Pad-foot) and SAKAI (Smooth drum) rollers exhibited more homogenous distribution of stiffness data with clear distinction of the weak areas.
- The data acquisition system (UTEP Sensors) developed in this study was utilized to collect vibration data parallel to the retrofit systems to evaluate the performance of retrofit kits during IC data collection process. The proper positioning of the accelerometers is crucial in capturing the proper vibration energy. Comparing the calculated CMVs in terms of cumulative distribution between the retrofit kit and UTEP Sensors shows that they are reasonably similar with minor differences. Such comparison shows the proper performance of retrofit kit in determining the stiffness values. It should be noted that the results of retrofit kit on SAKAI roller during the soils rodeo was not quite comparable to the results of other retrofit kit on HAMM and CAT rollers.
- The reported vibration frequencies from UTEP Sensors during the moving vibration tests were reasonably agreeing with those reported as the roller specifications. However, the captured amplitudes from UTEP Sensors were different from the nominal vibration amplitudes reported in the vendor specifications. Such differences could be dependent of the layer stiffness and roller speed during the operation.

References

Anderegg, R. (1998). "Nichtlineare Schwingungen bei dynamischen Bodenverdichtern (Nonlinear Vibrations with Dynamic Soil Compactors)." Eidgenössische Technishe Hochschule ETH Zürich, Zürich, Switzerland.

Anderegg, R., and Kaufmann, K. (2004). "Intelligent Compaction with Vibratory Rollers: Feedback Control Systems in Automatic Compaction and Compaction Control." *Transportation Research Record: Journal of the Transportation Research Board*, Transportation Research Board of the National Academies, 1868, pp. 124–134.

Ferris, A. J. (1985). "Developments in Compaction Control Systems." *Highways & Transportation*, 32(7), pp. 2–5.

Floss, R., Kröber, W., and Wallrath, W. (2001). "Dynamische Bodensteifigkeit als Qualitätskriterium für die Bodenverdichtung (Dynamic Soil Stiffness as a Quality Criterion for Soil Compaction)." 4. Internationales Symposium Technik und Technologie des Verkehrswegebaus (4th International Symposium and Technology Series of Transportation Infrastructures), BAUMA, München, Germany.

Mooney, M., and Adam, D. (2007). "Vibratory Roller Integrated Measurement of Earthwork Compaction: An Overview." In *FMGM 2007: Seventh International Symposium on Field Measurements in Geomechanics*, ASCE, pp. 1-12.

Mooney, M.A., Rinehart, R.V., Facas, N.W., Musimbi, O.M., White, D.J. and Vennapusa, P.K.R. (2010), "Intelligent Soil Compaction Systems," *NCHRP Report 676*, National Cooperative Highway Research Program, Transportation Research Board, Washington, D.C.

Nazarian, S., Mazari, M., Abdallah, I. N., Puppala, A. J., & Mohammad, L. N. (2014). "Modulus-Based Construction Specification for Compaction of Earthwork and Unbound Aggregate." *NCHRP 10-84 Final Report*, Center for Transportation Infrastructure Systems (CTIS), The University of Texas at El Paso, El Paso, TX.

Nazarian, S., Mazari, M., Chang, G., Aldouri, R., and Beltran J. (2015). "Intelligent Compaction Roller Retrofit Kit Validation." *Report FHWA TIDP-130(096)*, Center for Transportation Infrastructure Systems (CTIS), The University of Texas at El Paso, El Paso, TX.

Petersen, J. S., Romanoschi, S. A., and Hossain, M. (2007). "Development of Stiffness-Based Specifications for In-Situ Embankment Compaction Quality Control." Report No. K-TRAN: KSU-04-6. Kansas State University, Manhattan, KS.

Siddagangaiah, A.K., Aldouri, R., Nazarian,S., Chang,C.M., and Puppala, A. (2013). "Improvement of Base and Soil Construction Quality by Using Intelligent Compaction Technology." *Report FHWA/TX-13/0-6740-1*, Center for Transportation Infrastructure Systems (CTIS), The University of Texas at El Paso, El Paso, TX.

Tirado, C., Mazari, M., Carrasco, C., and Nazarian, S. (2015). "Evaluating Influence Depth of Light Weight Deflectometer through Finite Element Modeling." *Airfield and Highway Pavements 2015*, pp. 789-800.

Thurner, H. F., and Forsblad, L. (1978). "Compaction Meter on Vibrating Rollers." Research Bulletin Nr. 8022, Solna, Sweden.

Thurner, H. F., and Sandström, Å. (1980). "A New Device for Instant Compaction Control." *Proceedings of International Conference on Compaction*, Paris, France, pp. 611–614.

Vennapusa, P. K., White, D. J., and Morris, M. D. (2009). Geostatistical Analysis for Spatially Referenced Roller-Integrated Compaction Measurements. *Journal of Geotechnical and Geoenvironmental Engineering*, *136*(6), 813-822.

White, D. J., Vennapusa, P. K., and Thompson, M. J. (2007). "Field Validation of Intelligent Compaction Monitoring Technology for Unbound Materials." *Report MN/RC-2007-10*, Center for Transportation Research and Education (CTRE), Iowa State University, Ames, IA.

White, D. J., Thompson, M. J., Vennapusa, P., and Siekmeier, J. (2008). "Implementing Intelligent Compaction Specification on Minnesota TH-64 Synopsis of Measurement Values, Data Management, and Geostatistical Analysis." *Transportation Research Record, Journal of the Transportation Research Board*, (2045), pp. 1–9.

White, D.J. and Vennapusa, P.K.R. (2010), "A Review of Roller-Integrated Compaction Monitoring Technologies for Earthworks," *Final Report ER10-04*, Earthworks Engineering Research Center, Iowa State University, Ames, IA.

White, D. J., Vennapusa, P. K., and Gieselman, H. H. (2011). "Field Assessment and Specification Review for Roller-Integrated Compaction Monitoring Technologies." *Advances in Civil Engineering*, Vol. 2011.

Appendix A

Appendix A includes detailed information of the correlation analysis of spot tests and IC data on SH24 highway. The results of the spot test for every lift were correlated with the IC data collected during the construction of highway SH24. In order to correlate the IC data with the different spot tests, a buffer of three feet in radius for every spot test was made. All the IC measurement inside the three feet radius were averaged and correlated for every spot test

A.1 LIME TREATED SUBGRADE

Correlation between IC data and spot test collected during the construction on SH24 of LTS layer on August 12, 2015 are presented in this section. Figure A.1.1 through A.1.3 shows the correlation between CMV and spot test on LTS layer.

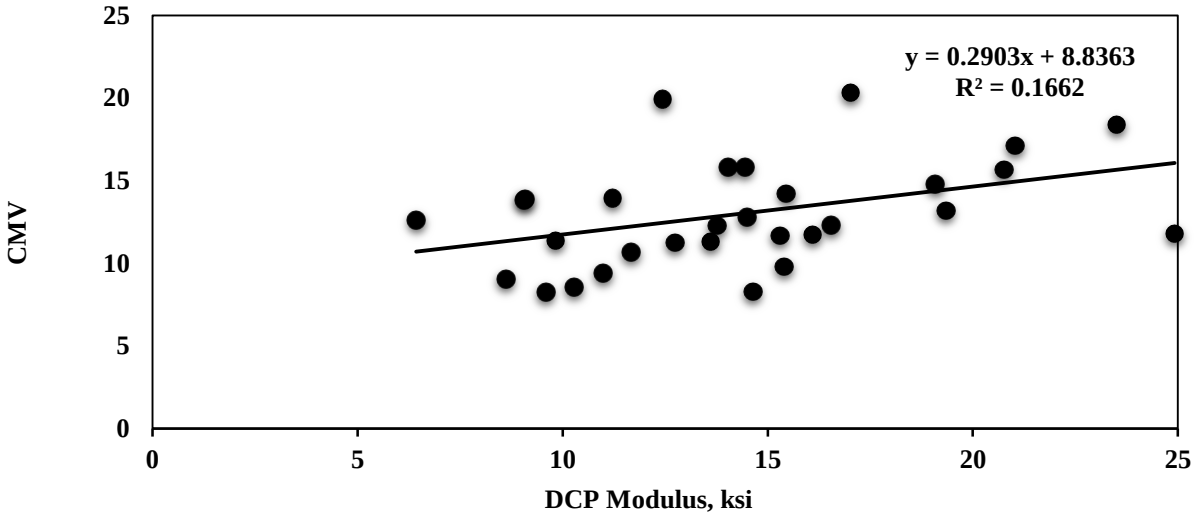

Figure A.1.1: Correlation between CMV and DCP on compacted LTS layer

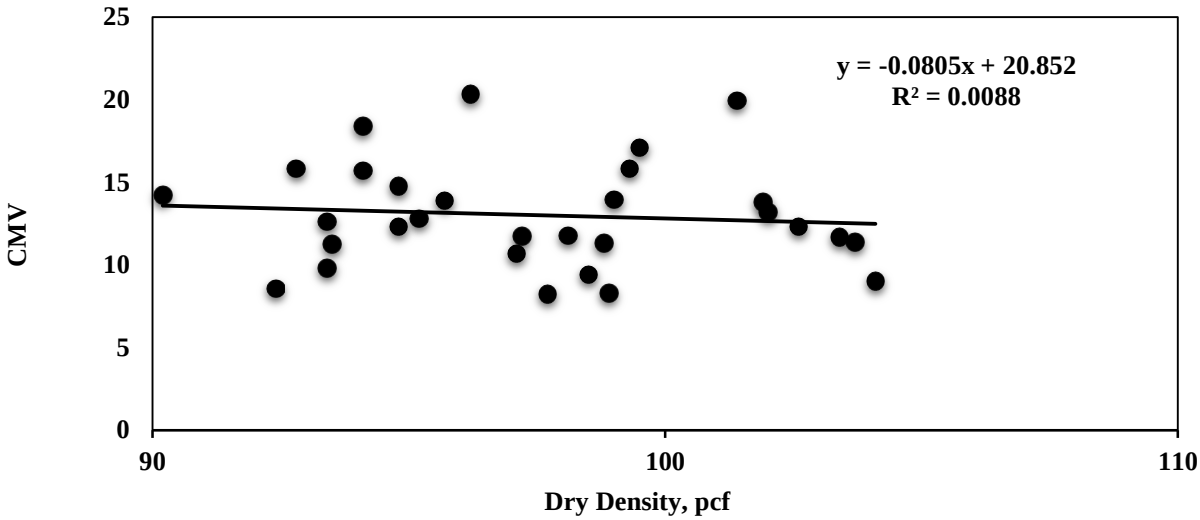

Figure A.1.2: Correlation between CMV and Dry Density on compacted LTS layer

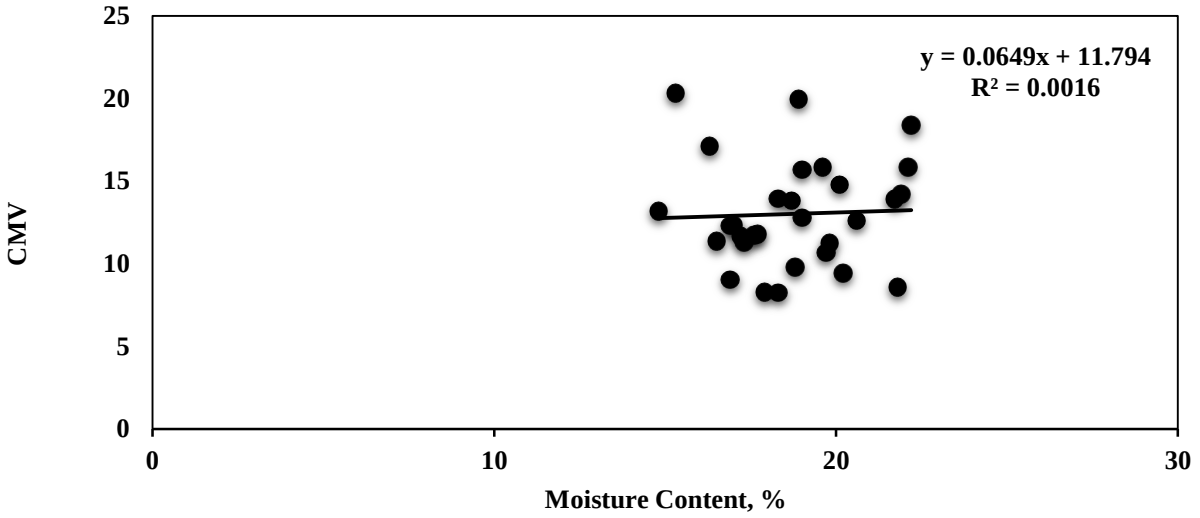

Figure A.1.3: Correlation between CMV and Moisture Content on compacted LTS layer

A.2 CEMENT TREATED BASE

Correlation between IC data and spot test collected during the construction on SH24 of CTB layer on September 4, 2015 are presented in this section. Figure A.2.1 through A.2.3 shows the correlation between CMV and spot test on CTB layer.

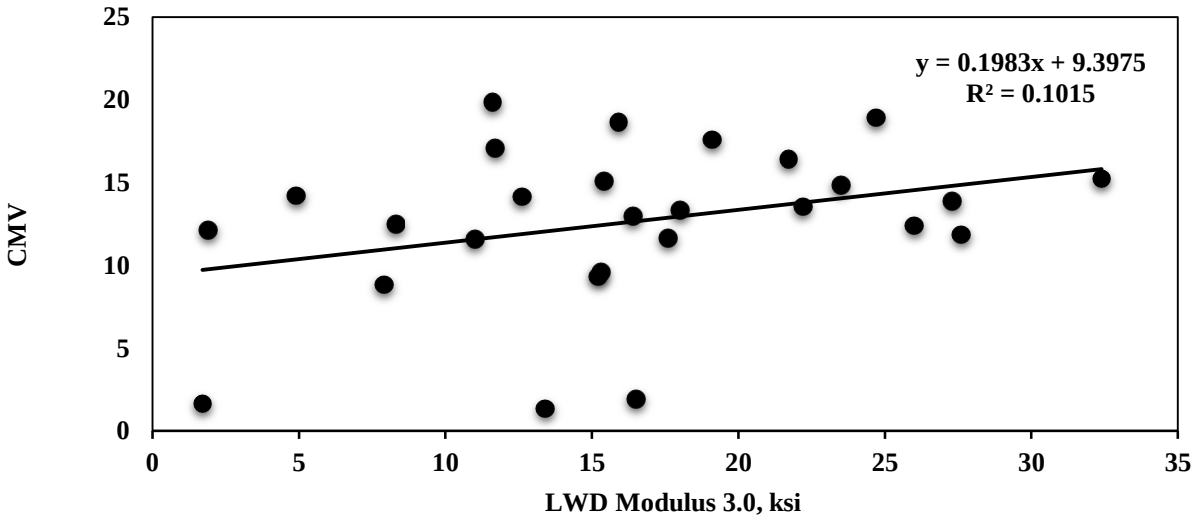

Figure A.2.1: Correlation between CMV and LWD (model 3.0) on compacted CTB layer

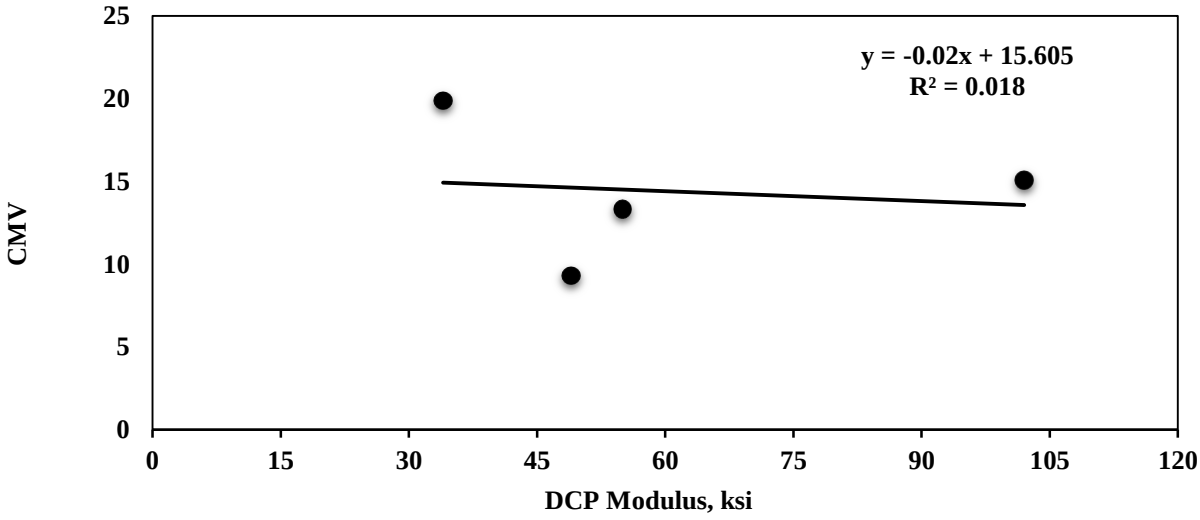

Figure A.2.2: Correlation between CMV and DCP on compacted CTB layer

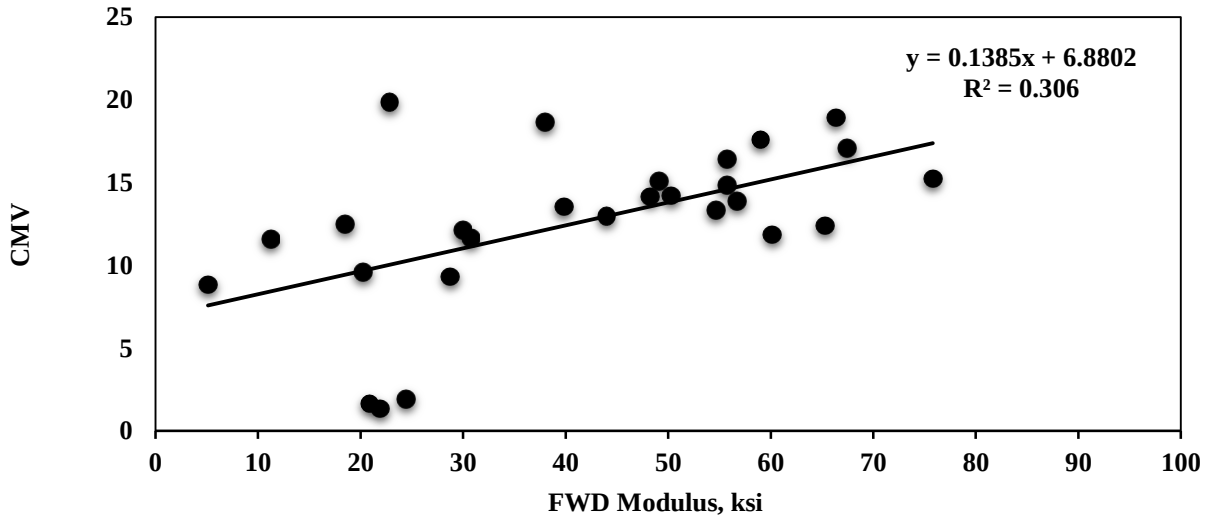

Figure A.2.3: Correlation between CMV and FWD on compacted CTB layer

A.3 FLEXIBLE BASE

Correlation between IC data and spot test collected during the construction on SH24 of FB layer on September 18, 2015 are presented in this section. Figure A.3.1 through A.3.4 shows the correlation between CMV and spot test on

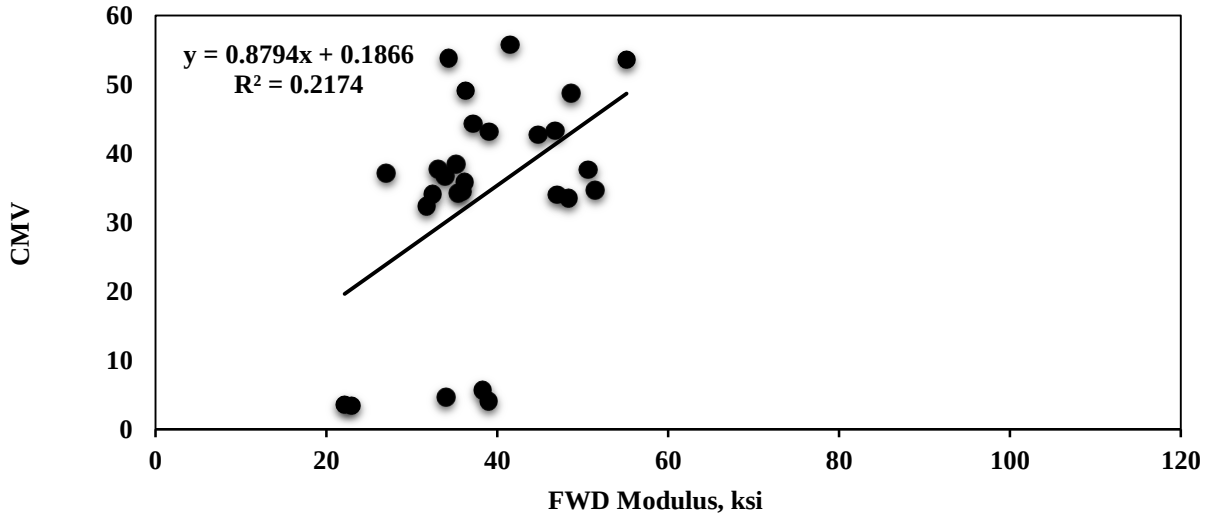

Figure A.3.1: Correlation between CMV and FWD on compacted FB layer

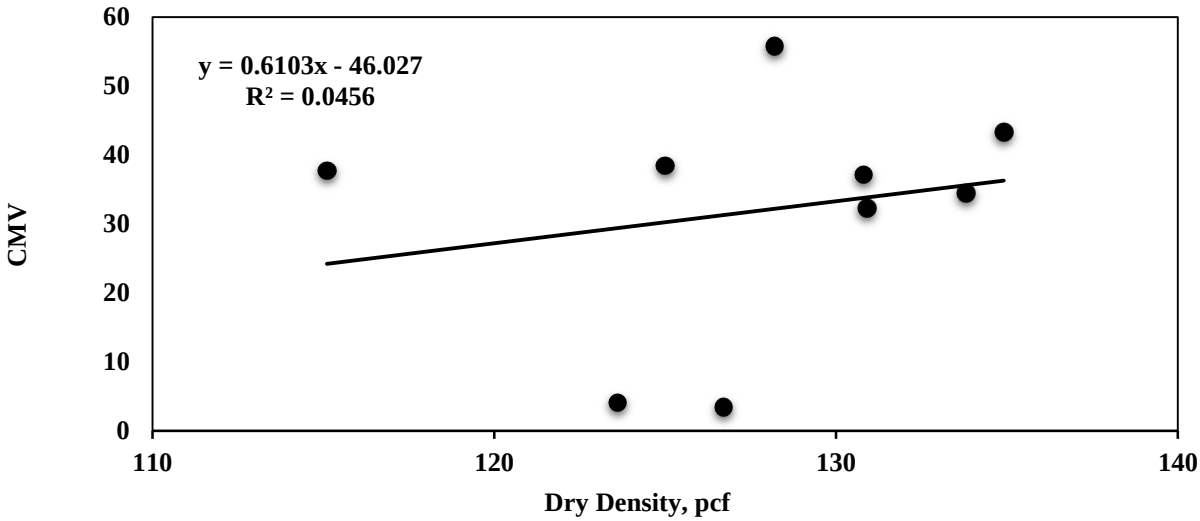

Figure A.3.2: Correlation between CMV and Dry Density on compacted FB layer

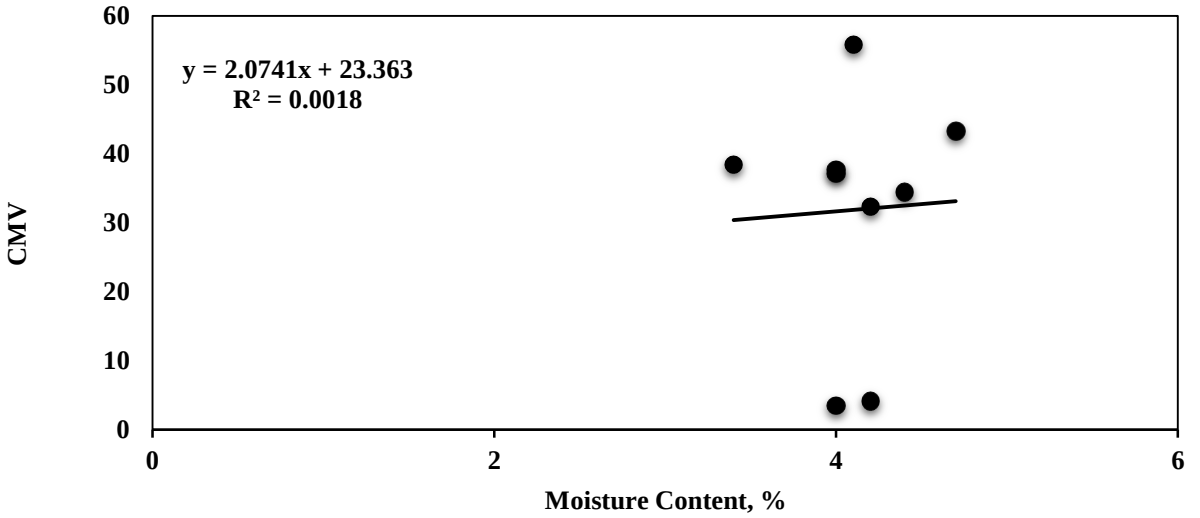

Figure A.3.3: Correlation between CMV and Moisture Content on compacted FB layer

No strong correlation between IC data and spot test were found in any of the three layer tested. This might be due to the different depth of influence of every device.

Appendix B

Appendix B includes detailed analyses of data collected with UTEP validation system in Cleburne TX.

B.1 VIBRATION EVALUATION DURING FIRST DAY OF COMPACTION

A spectrogram is a graph of the amplitude spectra accumulated at different times during the vibration of the drum. The forcing frequency of vibration is shown as the darkest strip in each spectrogram. Figure B.1.1 shows the spectrogram of vibration data during the second pass of HAMM roller at a higher frequency than the previous pass.

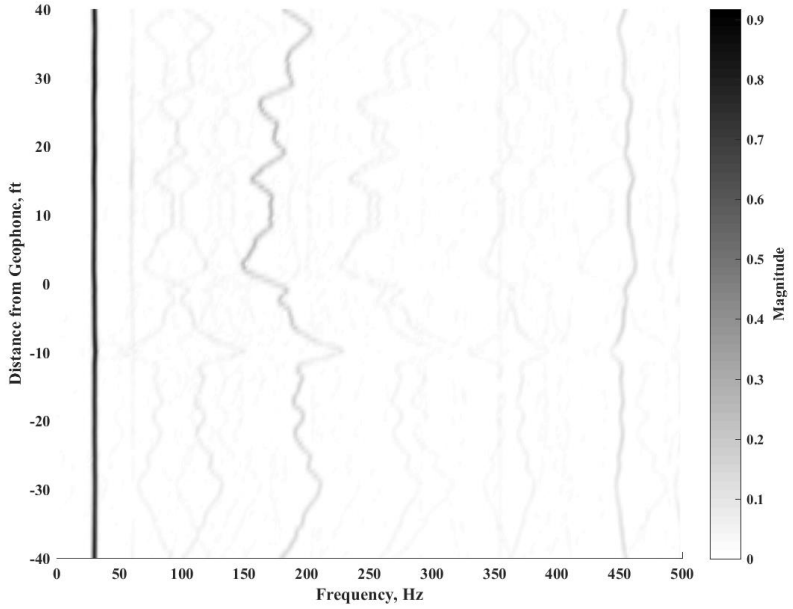

Figure B.1.1: Spectrogram of vibration data from mounted accelerometer for the second pass on HAMM roller (Nov.18)

Figure B.1.2 illustrates the spectrogram in the fifth pass at a forcing frequency of about 32 Hz on SAKAI roller. The second harmonic is not visible in this figure

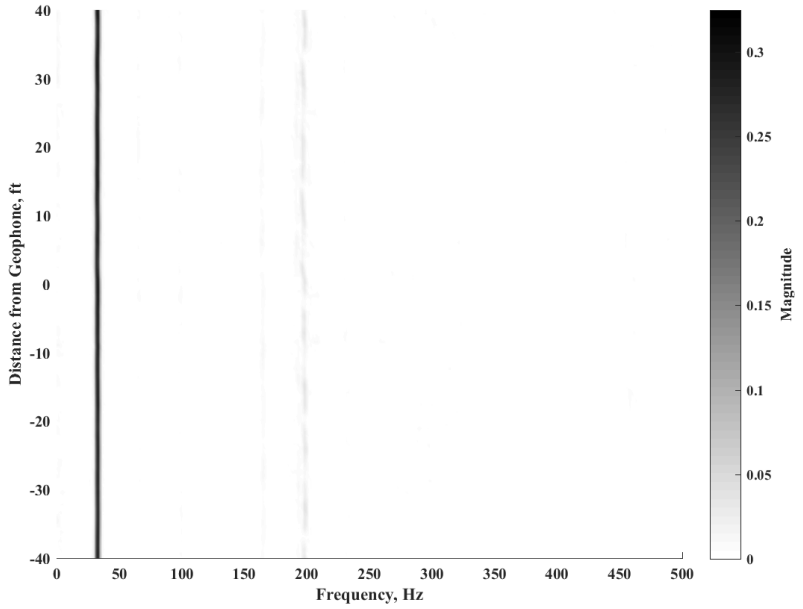

Figure B.1.2: Spectrogram of vibration data from mounted accelerometer for the fifth pass on SAKAI roller (Nov.18)

B.2 VIBRATION EVALUATION DURING SECOND DAY OF COMPACTION

As stated before, a clayey subgrade layer was placed, compacted and then mapped by three different IC rollers during the second day. The first eight passes were covered by HAMM and CAT rollers. SAKAI was the last roller used. It covered from the ninth to the twelfth pass. It should be noted that only SAKAI roller was instrumented with UTEP sensors during the subgrade compaction. Figure B.2.1 illustrates the average forcing frequency from the retrofit kit and UTEP sensors for SAKAI passes. In this figure, the average forcing frequencies are very similar on every pass for the retrofit and UTEP sensors. The average amplitudes corresponding to the forcing frequencies from SAKAI roller are the same between all passes. Figure B.2.2 represents the average amplitudes measured from the retrofit kit for each pass. The amplitudes shown for every pass is about one millimeter.

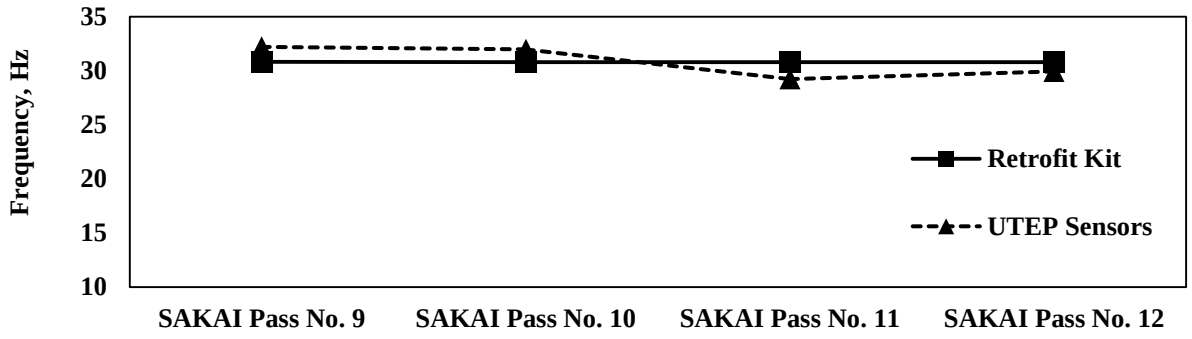

Figure B.2.1: Comparison of vibration frequency from retrofit kit and UTEP sensors on SAKAI roller between different passes (Nov.19)

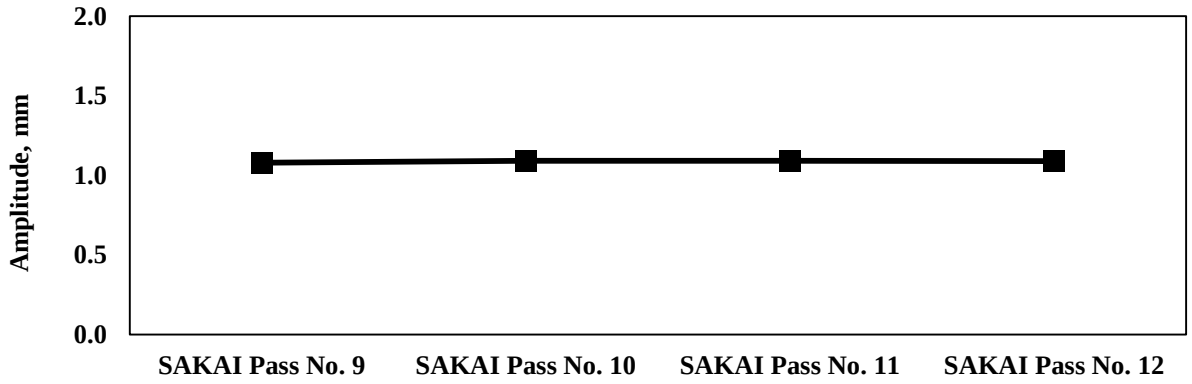

Figure B.2.2: Comparison of vibration amplitude from retrofit kit on SAKAI roller between different passes (Nov.19)

Figure B.2.3 shows the cumulative distribution of the CMV's from the retrofit kit on SAKAI rollers between the ninth and the twelfth pass. The CMV distributions for all the passes seems to have the same trend in this figure. Figure B.2.4 shows the cumulative distribution of the CMV's from the UTEP sensors on SAKAI rollers between the ninth and the twelfth pass. Even though, the CMV distribution from the UTEP sensors tends to be greater than the retrofit kit, they all seem to be very constant with no drastic changes on their CMV.

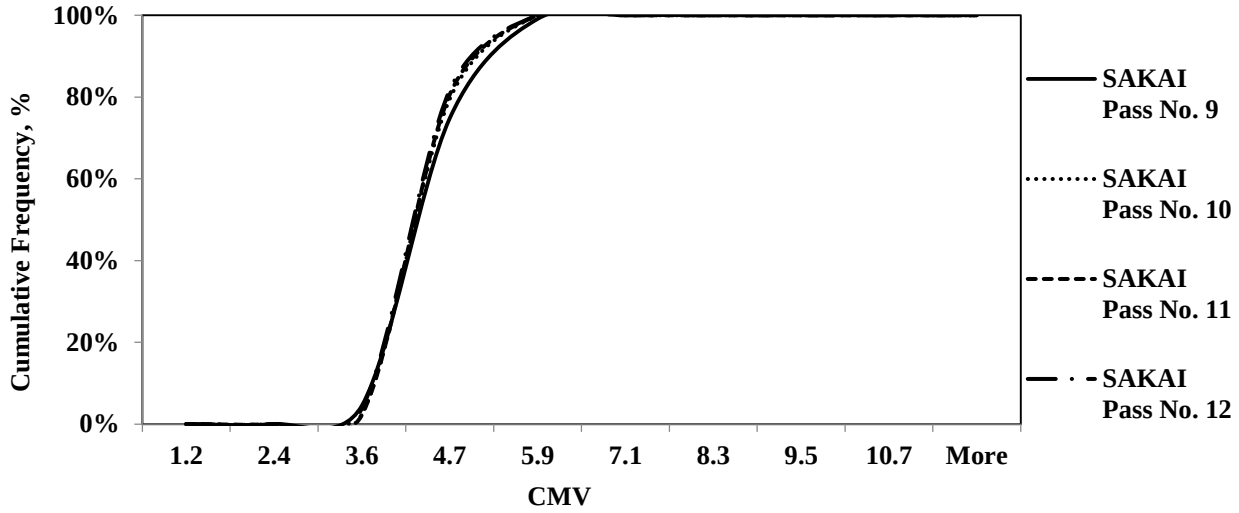

Figure B.2.3: Comparison of CMV data from retrofit kit on SAKAI roller between different passes (Nov.19)

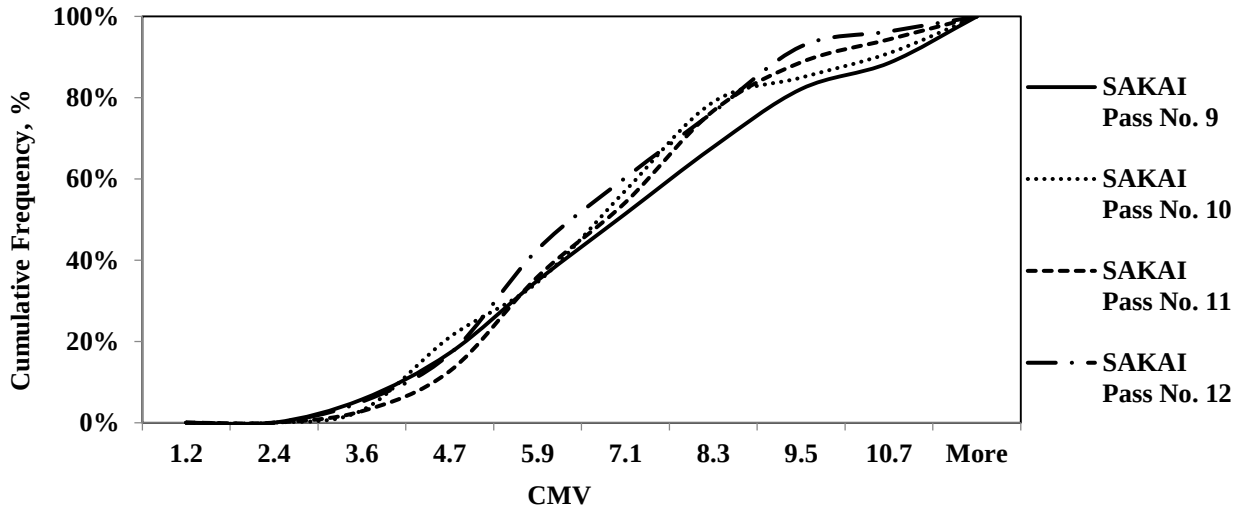

Figure B.2.4: Comparison of CMV data from validation system on SAKAI roller between different passes (Nov.19)

Figure B.2.5 compares the cumulative distribution of the CCV's from the UTEP sensors on SAKAI rollers between the ninth and the twelfth pass. The CCV distributions between the passes tend to decrease for every pass. Figure B.2.6 through B.2.9 illustrate the spectrogram of the vibration of the drum during the 9^{th} through 12^{th} passes on SAKAI roller at high frequency and low amplitude setting.

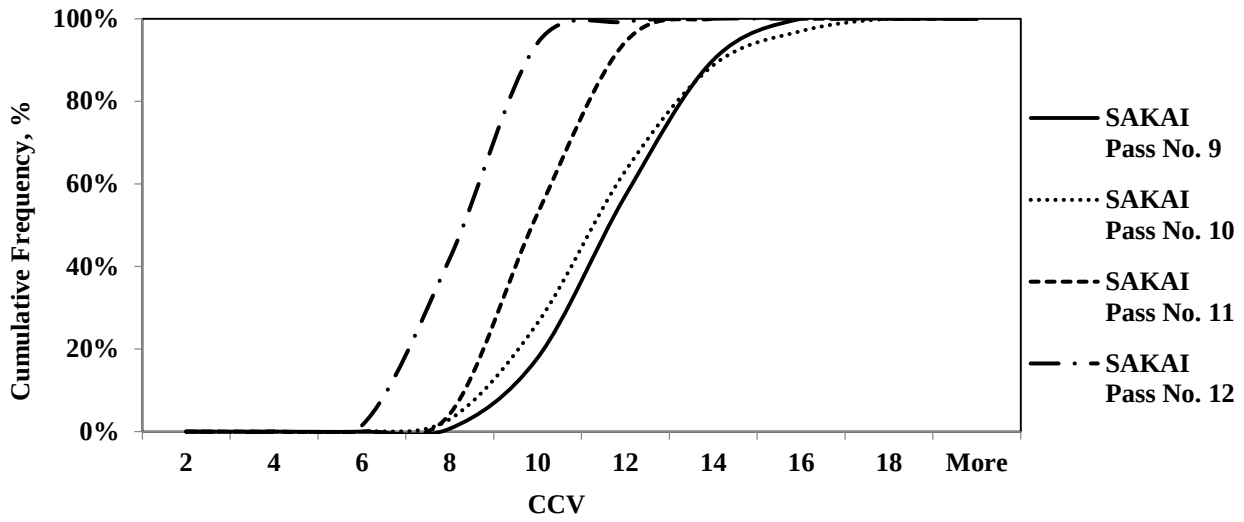

Figure B.2.5: Comparison of CCV data from retrofit kit on SAKAI roller between different passes (Nov.19)

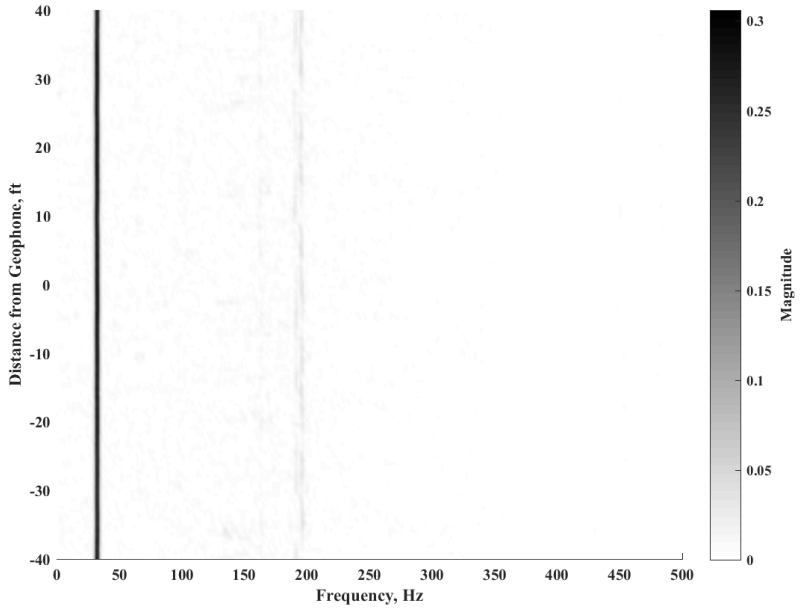

Figure B.2.6: Spectrogram of vibration data from mounted accelerometer for the 9th pass on SAKAI roller (Nov.19)

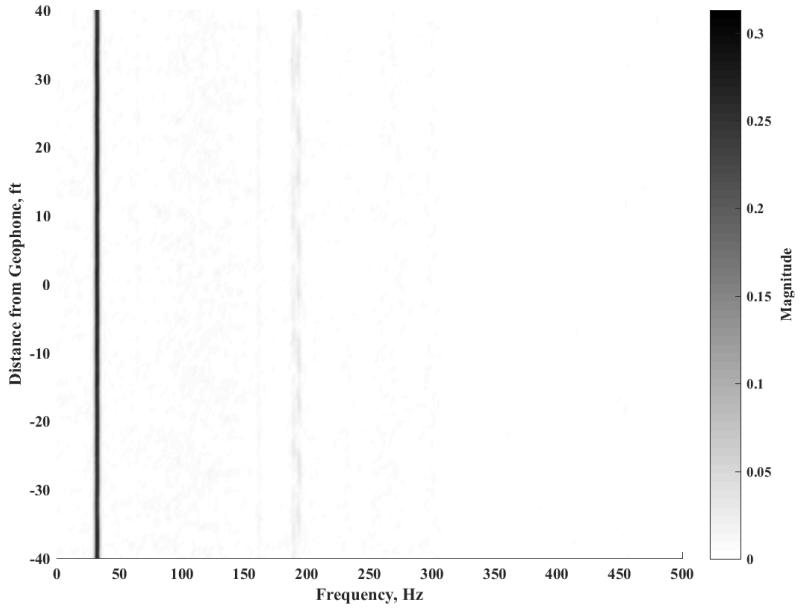

Figure B.2.7: Spectrogram of vibration data from mounted accelerometer for the 10th pass on SAKAI roller (Nov.19)

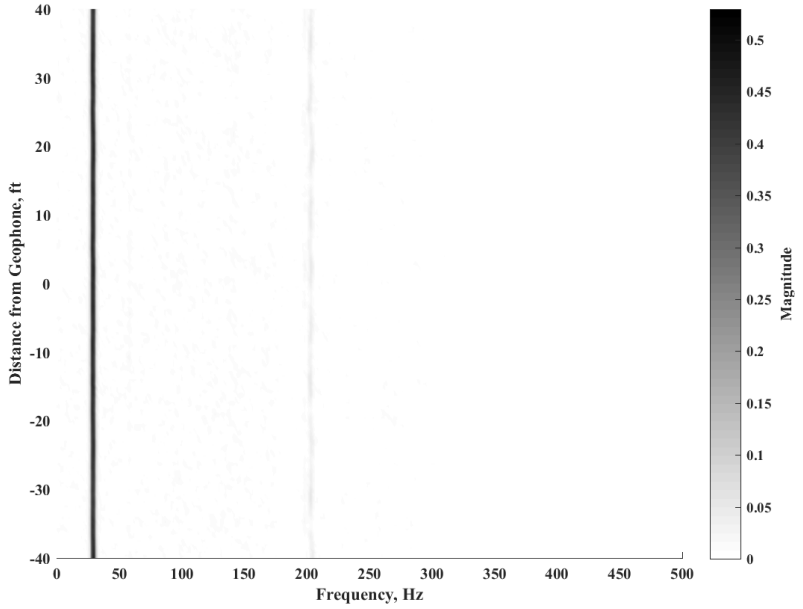

Figure B.2.8: Spectrogram of vibration data from mounted accelerometer for the 11th pass on SAKAI roller (Nov.19)

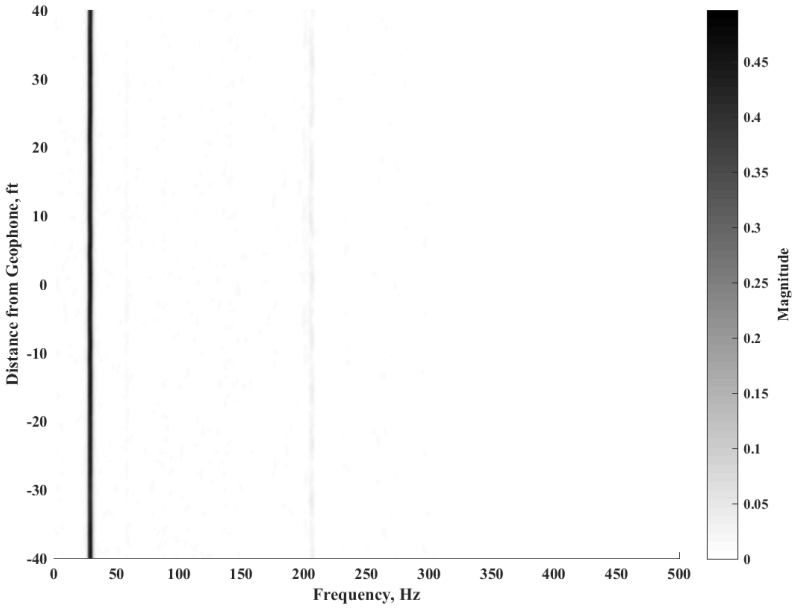

Figure B.2.9: Spectrogram of vibration data from mounted accelerometer for the 12th pass on SAKAI roller (Nov.19)

Vita

Jorge Beltran was born in Mexico, and pursued all his studies in Mexico until his high school graduation in 2007. He attended The University of Texas at El Paso to pursue a Bachelors in Civil Engineering. During his junior year he started to work at the Center for Transportation Infrastructure Systems. Here he got involved in multiple research project working with asphalt binder and hot mix asphalt with the chance to perform several laboratory tests. Right after his bachelors' graduation, Jorge decided to pursue a Master degree in the field of Geotechnical Engineering. During his graduate studies, he was involved in two research project sponsored by the Federal Highway Administration and the Texas Department of Transportation.

Permanent address: 716 Azurita.
Ciudad Obregon, Sonora, Mexico 85136

This thesis was typed by Jorge Beltran.